The Centromere–Kinetochore Complex: A Repeat Subunit Model

R. P. Zinkowski,* J. Meyne,‡ and B. R. Brinkley*

*Department of Cell Biology, University of Alabama at Birmingham, Birmingham, Alabama 35294; and ‡Genetics Group, Los Alamos National Laboratory, Los Alamos, New Mexico 87545

Abstract. The three-dimensional structure of the kinetochore and the DNA/protein composition of the centromere–kinetochore region was investigated using two novel techniques, caffeine-induced detachment of unreplicated kinetochores and stretching of kinetochores by hypotonic and/or shear forces generated in a cytocentrifuge. Kinetochore detachment was confirmed by EM and immunostaining with CREST autoantibodies. Electron microscopic analyses of serial sections demonstrated that detached kinetochores represented fragments derived from whole kinetochores. This was especially evident for the seven large kinetochores in the male Indian muntjac that gave rise to 80–100 fragments upon detachment. The kinetochore fragments, all of which interacted with spindle microtubules and progressed through the entire repertoire of mitotic movements, provide evidence for a subunit organization within the kinetochore. Further support for a repeat subunit model was obtained by stretching or uncoiling the metaphase centromere–kinetochore complex by hypotonic treatments. When immunostained with CREST autoantibodies and subsequently processed for in situ hybridization using synthetic centromere probes, stretched kinetochores displayed a linear array of fluorescent subunits arranged in a repetitive pattern along a centromeric DNA fiber. In addition to CREST antigens, each repetitive subunit was found to bind tubulin and contain cytoplasmic dynein, a microtubule motor localized in the zone of the corona. Collectively, the data suggest that the kinetochore, a plate-like structure seen by EM on many eukaryotic chromosomes is formed by the folding of a linear DNA fiber consisting of tandemly repeated subunits interspersed by DNA linkers. This model, unlike any previously proposed, can account for the structural and evolutional diversity of the kinetochore and its relationship to the centromere of eukaryotic chromosomes of many species.

THE kinetochore is a highly differentiated structure located at the centromere (primary constriction) of chromosomes and serves as an attachment site for spindle microtubules. Recent evidence suggests that kinetochores capture and stabilize microtubules that grow from the spindle poles (23, 36) and participate in the generation of forces necessary for chromosome movement in mitosis and meiosis (39, 49). In electron micrographs, the kinetochore typically appears as a triple-layered plate or disc situated at the sides of the centromere. Notable structural variations include the "ball and cup" kinetochores of many plant chromosomes and diffuse kinetochores of some plant and insect chromosomes (reviewed in references 12 and 48). Although many reports in the literature have described the ultrastructure of the kinetochore, considerable confusion still exists in the use of the terms centromere and kinetochore and how the structure and molecular composition of one relates to the other. Since the inner layer of the trilaminar kinetochore plate is juxtaposed to and intimately associated with centromeric chromatin fibers, this region of the chromosome appears to be integrated into a functional complex that ensures proper distribution of the genetic material.

Moroi et al. (38) have shown that serum from individuals with the CREST[1] (calcinosis, Raynaud's phenomenon, esophageal dysmotility, sclerodactyly, and telangiectasia) variant of scleroderma contains autoantibodies that bind to components of the centromere. This seminal discovery opened the way for the first significant immunocytochemical and biochemical analyses of the centromere-kinetochore region of eukaryotic chromosomes. Subsequently, immunoblots of nuclear proteins using CREST sera led to the discovery of several new centromeric polypeptides, including CENP-A (18 kD), CENP-B (80 kD), and CENP-C (140 kD) (20, 57). Using immunoperoxidase at the electron microscopic level, these proteins were detected on the inner and outer kinetochore plates and subjacent chromatin of mammalian chromosomes (4). More recently using immunogold EM probes, label was localized to the heterochromatin of human centromeres (19). Masumoto et al. (28) demonstrated that the alphoid DNA of the centromere contains specific sequences that interact with CENP-B. Earlier histocytochemical evidence indicates that kinetochores are composed of DNA (40,

1. *Abbreviations used in this paper*: CREST, calcinosis, Raynaud's phenomenon, esophageal dysmotility, sclerodactyly, and telangiectasia; HU, hydroxyurea; MUG, mitotic cells with unreplicated genomes.

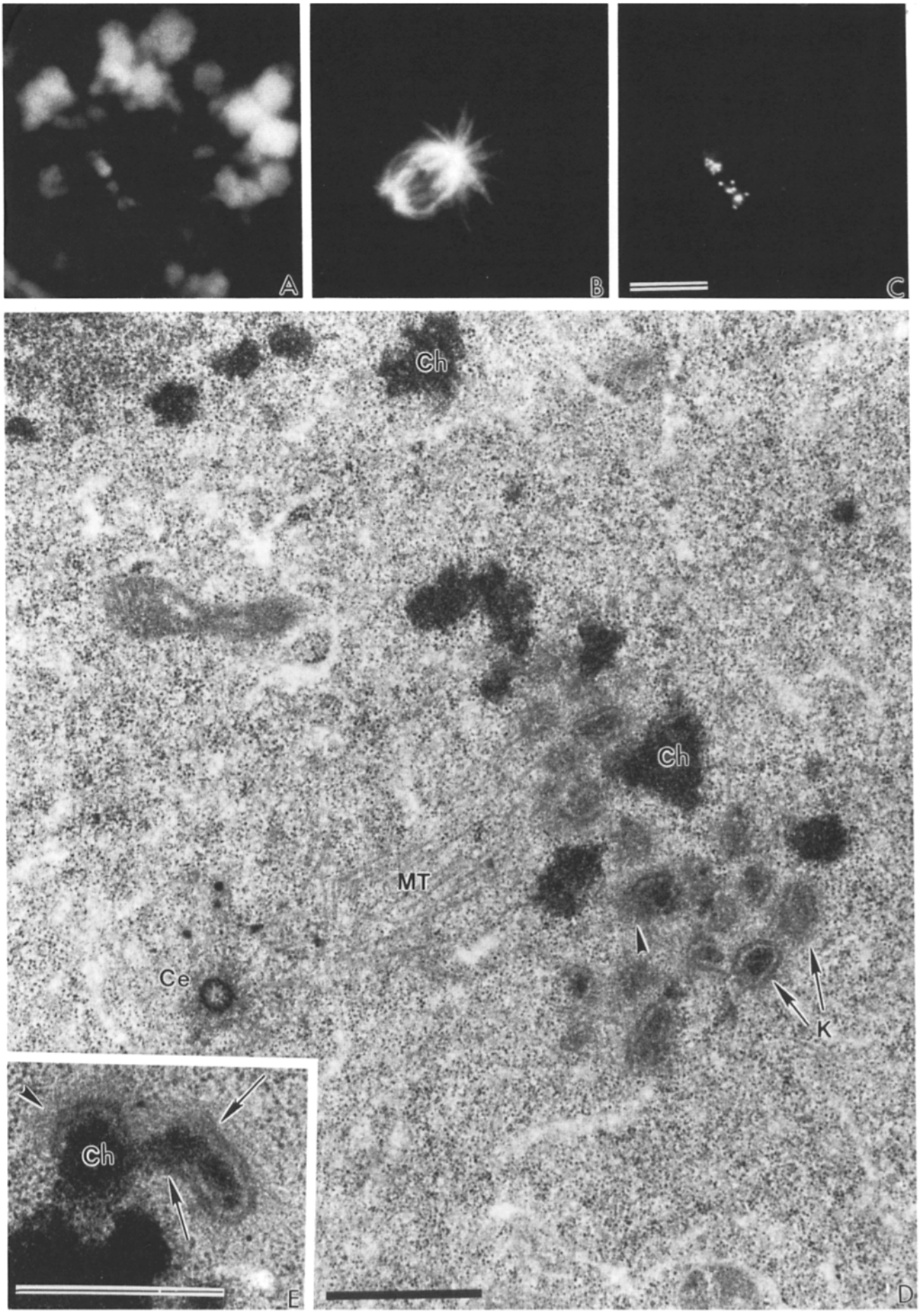
A
B
C
Ch
Ch
MT
Ce
K
Ch
D
E

46), protein (57), and possibly RNA (47), although the precise relationships of how these macromolecules relate to kinetochore ultrastructure is not well understood. Based largely on EM evidence, the kinetochore has been described as a proteinaceous plate formed or deposited near the centromere (13, 17, 51), a fiber composed of DNA complexed to protein (5, 6, 44, 46, 50), or a combination of both (50).

Knowledge of centromeric DNA and its contribution to the function and structure of the centromere–kinetochore comes largely from molecular genetics studies of yeast chromosomes. The centromeres of the budding yeast *Saccharomyces cerevisiae* are contained within a 220-bp nuclease resistant core region that is folded into a particle of 15–20 nm in diameter, which is capable of binding a single microtubule (reviewed in references 2 and 15). Within this core exists three regions of conserved homology, called centromere DNA elements, or CDE I, II, and III. CDE I (8 bp) and III (25 bp) consist of regions of conserved homology that are separated by CDE II (78–86 bp) that is composed primarily of A + T base pairs. All three CDEs are necessary for proper centromere function, and two of these elements, CDE I and III, associate with DNA binding proteins as demonstrated by gel retardation studies in vitro (21). Thus, the chromatin–protein complex that exists is *S. cerevisiae* centromeres may represent a primitive kinetochore. In contrast, the centromeres of the distantly related fission yeast *Schizosaccharomyces pombe* are larger and more complex. The smallest restriction fragments containing active centromeres are 65–150 kb in length and contain blocks of repetitive, heterochromatin-like, untranscribed DNA arranged in tandem arrays flanking a 7-kb central core (15, 16). Thus, centromeres of *S. pombe* more closely resemble their counterparts in higher eukaryotes such as mammals that contain heterochromatin and repetitive DNA, the major class being α-satellite, that extends for several megabases along the centromere (59, 60).

Although the centromeres of *S. cerevisiae* and *S. pombe* are well characterized at the DNA and genetic levels, details concerning proteins and ultrastructure are generally lacking in yeasts; the reciprocal is true of higher eukaryotic chromosomes. Here a discrete ultrastructure is observed and some of the proteins can be detected and analyzed by antikinetochore antibodies. Relatively little is known, however, about chromatin and DNA of the centromere-kinetochore region of higher eukaryotic chromosomes.

In the present study we have used two novel approaches, one involving caffeine-induced kinetochore detachment and the other, centromere stretching to investigate the three-dimensional structure and composition of the centromere–kinetochore region and its relationship to the rest of the chromosome. Our study has demonstrated that kinetochore organization mirrors the pattern of repetitive DNA found in the centromeres of higher eukaryotes. Evidence is presented that the kinetochore is assembled from repetitive subunits tandemly arranged on a continuous DNA/protein fiber. Each subunit is a complex of constitutive and facultative proteins and DNA that can function autonomously when experimentally detached from the chromosome. This model, which we term the repeat subunit model, can account for the structural and evolutional diversity of the kinetochore and its relationship to the centromere of eukaryotic chromosomes of many species.

Materials and Methods

Cell Culture

Chinese hamster ovary (CHO) cells were grown in McCoys 5A (Iwakata and Grace modification) supplemented with 10% CPSR-4 (Sigma Chemical Co., St. Louis, MO). Both Indian muntjac (*Muntiacus muntjac vaginalis*) and Chinese muntjac (*Muntiacus reevesi*) were grown in Ham's F-10 medium supplemented with 15% FBS (Gibco Laboratories, Grand Island, NY). HeLa cells were grown in DMEM supplemented with 10% FBS. All growth media were supplemented with 100 U/ml of penicillin, 100 μg/ml streptomycin (Gibco Laboratories), 2 mM L-glutamine, and 1 mM sodium pyruvate. The cells were maintained in a humidified 37°C incubator with an air-5% CO_2 atmosphere.

Generation of MUGs

The generation of mitotic cells with unreplicated genomes (MUGs) has been described in detail previously (11, 62, 63). Briefly, confluent CHO cells arrested in G_1 by contact inhibition and nutrient depletion were replated to a density of 1×10^6 cells/28 mm^2 in fresh media containing 2 mM hydroxyurea (HU). After 20 h, the media was replaced with fresh media containing 2 mM HU and 5 mM caffeine. Cells entered mitosis within 2–6 h and were harvested by mitotic shake-off which usually resulted in a mitotic index of 90–96% MUGs.

The generation of Chinese and Indian muntjac MUGs required longer treatments with HU and caffeine due to their longer cell cycles. After replating the confluent cells to a density of 1×10^6 cells/28 mm^2, the cells were incubated in fresh media containing 2 mM HU for 40 h. The media was then replaced with media containing 2 mM HU and 5 mM caffeine. Chinese muntjac MUGs usually appeared in sufficient quantities within 2–6 h; however, Indian muntjac MUGs required 12–20 h in the HU–caffeine mixture before enough cells were obtained for slide preparations. In both cases, the MUGs were selectively detached by mitotic shake-off.

Mitotic Cell Preparation

Chromosomes from cultured cells were obtained by exposing the cultures to 0.1 μg/ml colcemid (Gibco Laboratories) or nocodazole (Sigma Chemical Co.) for 4–16 h. Mitotic cells were selectively detached from the substrate by lightly tapping the side of the flask. The cells were pelleted in a tabletop centrifuge at 1,000 *g* for 5 min and washed twice in PBS (0.14 M NaCl, 2.5 mM KCl, 8 mM Na_2HPO_4, 1.6 mM KH_2PO_4; pH 7.4).

Centromere Stretching

Stretching of centromeres of metaphase chromosomes was achieved by mechanical or hypotonic treatments. Mechanical stretching of chromosomes was achieved by resuspending the cell pellet in 1–2 ml of PBS. In some experiments, the cells were lysed by running the suspension forcibly through a 26-gauge syringe needle three times. In these instances, the cell suspension contained a protease inhibitor cocktail consisting of 0.1 mM PMSF and 1 μg/ml each of chymostatin, leupeptin, antipain, and pepstatin (P-CLAP). Approximately 100 μl of the cell suspension was placed into a cytocen-

Figure 1. Immunofluorescence and EM micrographs of CHO MUGs. Double-label immunofluorescence of a MUG stained with (*A*) Hoechst 33258 for DNA, (*B*) TU-27B for microtubules, and (*C*) CREST for kinetochores. The highly fragmented chromatin was typically found in the periphery of the cell, whereas detached kinetochores were aligned on the spindle. (*D*) EM micrograph of a cell similar to the one in *A–C*. The detached kinetochores (*K, arrows*) interacted with spindle microtubules (*MT*), that are continuous with the centrosome (*Ce*). Chromatin fragments (*Ch*) seen in the vicinity of the detached kinetochores lacked microtubule attachments as determined by serial section EM. (*E*) A kinetochore still partially attached to a large chromatin fragment. The kinetochore "plate" appears broken and discontinuous (*arrows*). Arrowheads in *D* and *E* point to the corona. Bars: (*C*) 5 μm; (*D* and *E*) 1 μm.

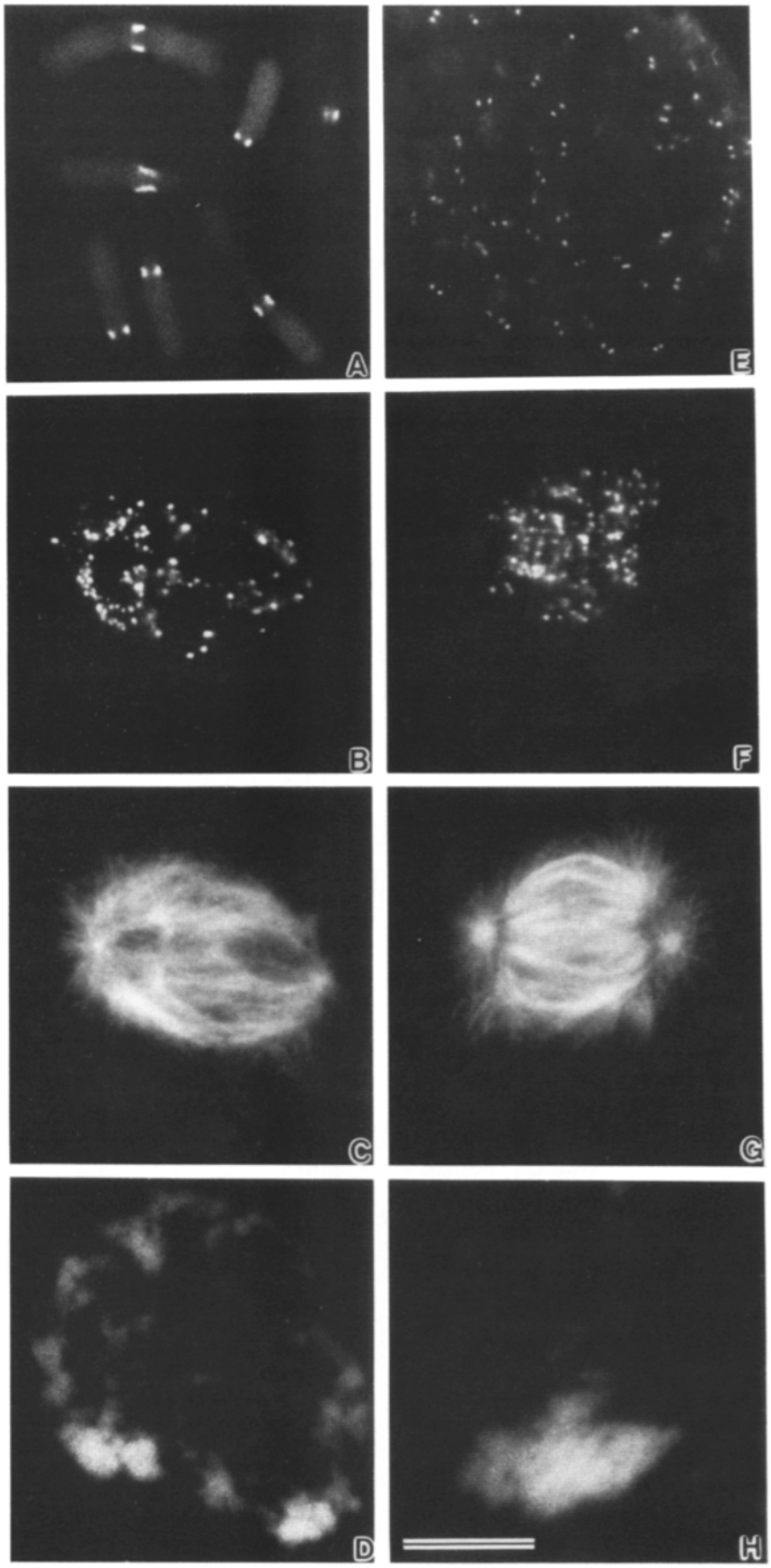

Figure 2. Kinetochores of normal and MUG muntjacs. Normal kinetochores visualized by CREST staining are shown for the Indian muntjac (*A*) and the Chinese muntjac (*E*). (*B–D*) Indian muntjac MUG stained for kinetochores (*B*), microtubules (*C*), and DNA (*D*). (*F–H*) A Chinese muntjac MUG stained for kinetochores (*F*), microtubules (*G*), and DNA (*H*). Both species of MUGs displayed 80–100 kinetochore fragments (*B* and *F*), that interacted with spindle microtubules (*C* and *G*) and contained pulverized chromatin (*D* and *H*) that was displaced to the periphery of the cell. Bar, 10 μm.

trifuge cup and spun onto a clean glass microscope slide or coverslip at 2,000 rpm for 2 min using a Cytospin (Shandon Instruments, Inc., Pittsburgh, PA) set at high acceleration.

Hypotonic stretching of chromosomes was achieved by resuspending the cell pellet in deionized dH_2O containing P-CLAP for times ranging from 1 to 9 min and then cytospun onto glass slides as described above. Generally, the longer the chromosomes were exposed to hypotonic solution, the more they were stretched.

Endosperm chromosomes from the plant *Haemanthus katherinae* Bak. were prepared as previously described (37). Some of the chromosomes in these preparations fortuitously became "mechanically" stretched due to shear forces generated during cytocentrifugation.

Tubulin Purification

Tubulin was purified by phosphocellulose chromatography from twice-cycled bovine brain microtubules as originally described by Mitchison and Kirschner (34). The critical concentration for spontaneous assembly of the purified 6S tubulin was 2.5 mg/ml, as determined by recording absorbance changes at 320 nm as the samples in microtubule assembly buffer PEM (80 mM Pipes, 1 mM EGTA, 1 mM $MgCl_2$, pH 7.2) with 1 mM GTP (PEM-G) were warmed from 4°C to 37°C as previously described (40).

Tubulin Lamination Of Kinetochores

For these experiments, exogenous bovine brain 6S tubulin protein was used. Colcemid-arrested cells that were washed free of the drug were resuspended in PBS supplemented with P-CLAP, lysed by passing the cells three times through a 26-gauge syringe needle, and then cytocentrifuged onto 20 × 10-mm glass coverslips as described above. The coverslips were subsequently immersed in PEM, followed by 0.05% Triton X-100 in PEM for 90 s, and then washed in three rinses of PEM. Lamination of kinetochores with tubulin was achieved by incubating the coverslips with 6S tubulin in PEM-G using concentrations at or below the critical concentration required for spontaneous assembly for 15 min at 37°C. The coverslips were then briefly rinsed three times in PEEM (0.1 M Pipes, pH 6.9, 1 mM $MgSO_4$, 0.1 mM EDTA, and 2 mM EGTA) at 37°C to remove the unpolymerized tubulin and stabilize the bound tubulin and microtubules. The coverslips were then immersed in 100% methanol at −20°C for 7 min or alternatively, in 2% EM grade formaldehyde (Tousimis Research Co., Rockville, MD) in PBS for 45 min at room temperature. The coverslips were then transferred to PBS and processed for indirect immunofluorescence as described below. Methanol fixation was preferred since it resulted in less background immunofluorescence.

Indirect Immunofluorescence

To visualize the centromere-kinetochore region of chromosomes, preparations were incubated with CREST serum SH diluted 1:100 in PBS, with the exception of *Haemanthus* endosperm, which was incubated with CREST serum EK at a dilution of 1:10 in PBS. Preparations were then stained with goat anti-human IgG conjugated to FITC (1:20 dilution; Boehringer Mannheim, Indianapolis, IN).

For double-label indirect immunofluorescence, formaldehyde-fixed preparations were blocked in 0.5 μg/ml $NaBH_4$ in PEM for 10 min, then TBS (0.05 M Tris base, 0.9% NaCl, pH 8.2) for 2 min and finally in PBS with 1% BSA (wt/vol) for 30 min. Methanol-fixed preparations were blocked in the PBS–BSA mixture only. The following combinations of antibodies were used in sequential order: Kinetochore/tubulin staining: SH CREST (1:100), goat anti-human IgG conjugated to biotin (1:20; Boehringer Mannheim), streptavidin Texas Red (1:200; Boehringer Mannheim), microtubule antibody Tu 27B (1:40, a gift from L. I. Binder, University of Alabama at Birmingham), sheep anti-mouse IgG-FITC (Accurate Chemical and Scientific Corp., Westbury, NY), rabbit anti-sheep IgG FITC (Accurate Chemical and Scientific Corp.). Kinetochore/dynein staining: Anti-dynein 70.1 (1:4, a gift from E. R. Steuer and M. P. Sheetz, Washington University School of Medicine, St. Louis, MO), goat anti-mouse IgM FITC (Boehringer Mannheim), rabbit anti-goat IgG $F(ab)^2$ (Fisher Scientific, Pittsburgh, PA), SH CREST, goat anti-human IgG biotin, avidin Texas Red. In all cases, antibodies were diluted in PBS containing 1% BSA and antibody incubations were for 30 min at 37°C. Each incubation was followed by three washes in PBS-BSA for 5 min each. All preparations were counterstained with 1 μg/ml Hoechst 33258 (Sigma Chemical Co.) in PBS for 5 min, rinsed in PBS, mounted in 1 mg/ml *p*-phenylenediamine in a 1:10 (vol/vol) mixture of PBS:glycerol, and sealed with nail polish.

In Situ Hybridization and CREST Staining

Cytospin preparations of normal or hypotonically stretched chromosomes were prepared, fixed, and CREST-stained by indirect immunofluorescence as described above. The preparations were photographed, and the microscope stage coordinates of each cell were recorded. The coverslips were removed and the slides were rinsed in 5 washes of PBS for 3 min each. The cells were post-fixed for 30 min in a 3:1 mixture (vol/vol) of methanol/glacial acetic acid and air dried. The cells were processed for in situ hybridization and the same cells were relocated and photographed.

In situ hybridization on HeLa cells was performed using a synthetic consensus sequence probe for alpha satellite DNA (30). In situ hybridization on CHO cells was performed using the telomere probe $(TTAGGG)_n$, which also hybridizes to tandem repeats of this sequence at the centromeres of most CHO chromosomes (31, 32). All in situ preparations were counterstained with 0.5 μg/ml propidium iodide and 0.06 μm/ml 4'6-diamidino-2-phenylindole (DAPI) in antifade solution.

Electron Microscopy

Cultured cells were harvested and collected as pellets or fixed in situ for 1.5 h in 3% glutaraldehyde in Millonig's phosphate buffer. The pellet or monolayer was washed three times in buffer and postfixed in 1% OsO_4 for 1.0 h. Subsequently, the cells were washed in 30% ethanol and stained en bloc with 2% uranyl acetate in 30% ethanol and dehydrated through a series of graded alcohols. The pellet was embedded in Spurrs plastic resin in BEEM capsules while cell monolayers were flat-embedded according to the procedure of Brinkley and Chang (7). Serial sections were cut on a diamond knife using an Ultracut E microtome (Reichert, Vienna, Austria), collected on formvar-coated slot grids (Ted Pella, Reading, CA) and stained with uranyl acetate followed by lead citrate. Care was taken to select ribbons of sections that were contiguous and displaying refractive colors of gray silver. Electron micrographs were taken on a Hitachi H-7000 electron microscope operated at 75 kV and images were recorded on Kodak sheet film for EM.

EM Morphometrics

Computer-assisted analysis of serial sections of chromosomes and kinetochores was accomplished using a PC-based software package described by Young et al. (61). Micrographs of serial sections were traced so that the digitizing tablet generated a digital image of each chromosome or kinetochore and morphometric data was recorded automatically as each structure was digitized.

Computer-enhanced Video Microscopy and Image Analysis

Computer-enhanced video microscopy and image analysis was performed using a Nikon Optiphot microscope equipped with epifluorescence and a DAGE MTI series 65 SIT video camera (Dage-MTI, Michigan City, IN) coupled to an Image 1-AT (Universal Imaging, Media, PA) image analysis system. Specially constructed filter cubes manufactured by Omega Optical, Inc. (Brattleboro, VT) for FITC (excitation filter = 485 nm, barrier filter = 530 nm) and Texas Red (excitation filter = 560 nm, barrier filter = 635 nm) eliminated the detection of false signals between the two fluorochromes. For image enhancement, gain and black level were set both on the camera and computer to provide an optimal signal. Then 128 video frames were summed into the foreground buffer, the image was defocused, and an additional 128 frames were summed into the background buffer. The background buffer was subtracted from the foreground buffer, subjected to contrast enhancement, and stored on the computer hard drive. Overlays of double fluorescence staining were achieved by aligning discernable fiduciary points within the images using the "subtract with shear" function. After alignment, the images in the frame buffers were superimposed using the "display RGB image" function, which pseudocolors images in the foreground and background buffers as red and green, respectively.

Image 1-AT was calibrated in the x and y axis using a stage micrometer. Lengths of CREST-stained kinetochores were measured using the "measure curvature length" function. The fluorescence areas of kinetochores were measured by summing 128 video frames using the "acquire image" function, the image was defocused and 128 frames were summed using the "acquire reference image" function, which was automatically subtracted from the acquired image. The image was then enlarged 2× using the "zoom" function and manually thresholded; the area was measured using the object measurement mode. All data was recorded to the hard drive and statistics were performed using Sigmaplot (Jandel Sciences, Corte Madera, CA).

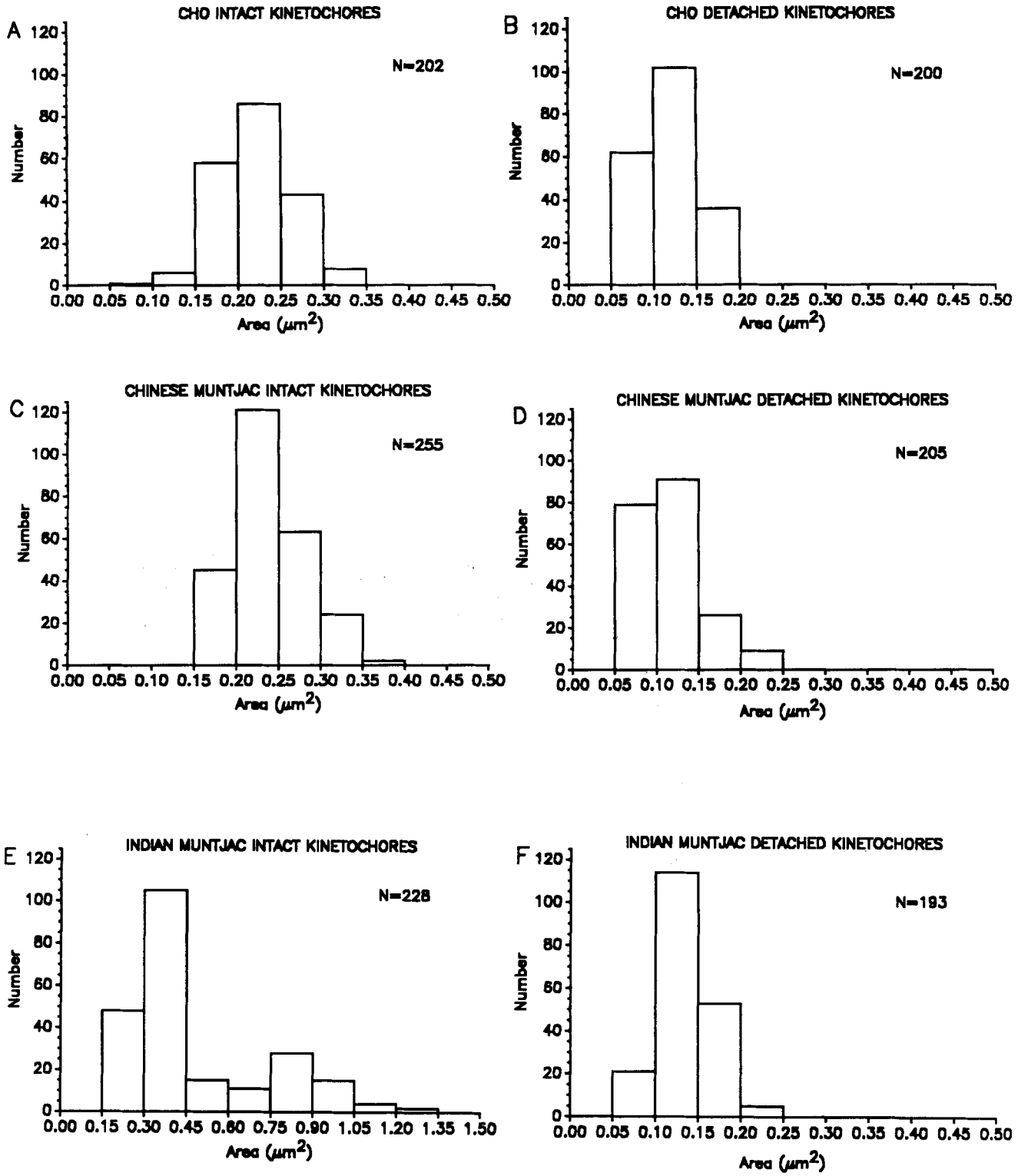

Figure 3. Digital image analysis of fluorescence areas of intact and detached kinetochores. Histograms of the distributions of fluorescent areas of CREST-stained intact kinetochores (*A*, *C*, and *E*) and detached kinetochores (*B*, *D*, and *F*) in CHO, Chinese muntjac, and Indian muntjac, respectively. Due to the large size of the Indian muntjac kinetochores the abscissa in *E* has been expanded.

Photography and Photomicroscopy

Computer-enhanced video microscope images were obtained using either a Kodak SV-65 or Sony UP-5000 color video printer. Photomicroscopy was performed using a Leitz Orthoplan epifluorescence microscope equipped with a Vario-orthomat 2 camera. Kodak T-Max 400 film was shot at ASA 1600 and push-processed in Kodak T-Max developer (9 min at 70°F).

Patient Sera

CREST sera S. H. and E. K. were obtained from the Comprehensive Arthritis Center at the University of Alabama at Birmingham; these sera have been previously characterized elsewhere (1, 33, 37).

Results

Detached Kinetochores of CHO MUGs

The mitotic apparatus (centrosomes, chromosomes, and spindle microtubules) is essential for the partitioning of genetic material to the daughter cells during mitosis and has been subject to detailed investigations by those studying cell division. Certain mammalian cell lines including Chinese hamster ovary (CHO) can be chemically induced to enter mitosis prematurely (53). We were interested in the mitotic apparatus of these cells and hence used immunofluorescence and EM techniques to study their morphology.

When CHO cells were synchronized at the G_1/S boundary of the cell cycle with 2 mM hydroxyurea (HU) for 20 h and subsequently exposed to 5 mM caffeine, the cells prematurely entered mitosis in the absence of DNA replication as previously reported (11, 53, 54). Since these cells entered mitosis without completing DNA synthesis, we refer to them as mitotic cells with unreplicated genomes (MUGs). When CHO MUGs were stained by indirect immunofluorescence using CREST autoantibodies, tubulin antibodies and Hoechst 33258, highly fragmented chromosomes were found dispersed throughout the cell (Fig. 1 *A*), whereas the kinetochores (Fig. 1 *C*), now detached from the rest of the genome, were found associated with the spindle microtubules (Fig. 1 *B*). As shown by Hoechst or propidium iodide staining, the detached kinetochores contained a residual amount of DNA (compare Figs. 1, *A* and *C*).

The kinetochores on CHO metaphase chromosomes are similar to other mammalian kinetochores and display a characteristic trilaminar morphology that has been extensively described in the recent literature (reviewed in 10, 12, 48). When MUGs were sectioned and examined by transmission electron microscopy (TEM), numerous profiles of kinetochores were morphologically similar to their counterparts on normal metaphase chromosomes. The striking difference, of course, was that kinetochores of MUGs were detached and displaced from the chromatin mass (Fig. 1 *D*, *arrows*). In most cells, kinetochores were attached to microtubules and aligned on the metaphase spindle (Fig. 1 *D*). Most of the chromatin fragments, however, remained displaced in the cytoplasm.

In most profiles, individual kinetochores consisted of a single-layered "plate" encompassing an electron dense chromatin core (Fig. 1 *D*, *arrows*). The structure of the plate was much like that described for the outer layer of intact kinetochores (5, 6, 17, 50), often appearing in individual sections as a pair of cohelically wound filaments ~5–10 nm in thickness. The plate was separated from the underlying chromatin by a less dense space of 25–30 nm in thickness. A fibrous corona extending from the kinetochore plate formed a fuzzy coat along the cytoplasmic surface of the detached kinetochores (Fig. 1, *D* and *E*, *arrowheads*). In both untreated or colcemid-arrested MUGs, most of the kinetochores were detached and completely displaced from the rest of the chromatin. In a few cells, however, kinetochores were still partially attached to large chromatin fragments and the kinetochore plate appeared to be broken and discontinuous (Fig. 1 *E*, *arrows*).

Movement and alignment of detached kinetochores required intact microtubules that extended from the centrosomes and attached to kinetochores in much the same way as in normal mitosis (Fig. 1 *D*). Microtubules usually terminated at the outer surface of the kinetochore plate as seen in serial section TEM. At metaphase, detached kinetochores were either bi- or mono-oriented within the same cell. When microtubules were attached to opposite sides of a detached kinetochore, it became bi-oriented to opposite poles, whereas kinetochores with microtubules extending from only one pole were mono-oriented.

Kinetochore Number Paradox of CHO MUGs

We were interested in determining the period of the cell cycle when CHO kinetochores became duplicated. If this event occurred at the G_1/S border, then cells blocked at this phase of the cell cycle with HU would be expected to possess replicated kinetochores. To determine when kinetochores in CHO cells became duplicated, immunofluorescence staining with CREST autoantibodies for kinetochore detection and single cell cytometry to measure DNA content of Hoechst 33258-stained cells was performed. It was found that kinetochores of CHO cells were duplicated when the DNA content was near or equal to 4C, thus indicating that the kinetochores replicated in late S or G_2 of the cell cycle (data not shown). This is in agreement with previous reports that demonstrate kinetochore duplication in late S or G_2 of the cell cycle in the cell lines of PtK_2 (male rat kangaroo) (4) and GLC1 (human tumor) (22), as well as the fungus *Saprolegnia* (24).

As we have shown previously, MUGs have a 2C DNA content and fail to progress through S phase (11), a prerequisite for normal kinetochore duplication. However, when the number of kinetochores were counted in each cell, most CHO MUGs were found to have a quasidiploid complement of kinetochores as detected by CREST immunofluorescence. This finding, although somewhat unexpected, suggested one of three possible explanations: (*a*) most of the cells were tetraploid, or (*b*) centromere-kinetochore DNA replication was resistant to the HU block and was completed before mitosis, or (*c*) kinetochores became fragmented into smaller functional subunits. A simple analysis of the karyotype of the CHO cells used in our experiments ruled out the possibility of tetraploidy. Therefore, we investigated the possibility that the DNA of the centromere–kinetochore region in MUGs could undergo replication in the presence of the HU block. To achieve this, CREST indirect immunofluorescence was combined with in situ autoradiography to detect tritiated thymidine incorporation in the detached kinetochores and associated chromosome fragments. This technique permitted the simultaneous observation of kinetochores by fluorescence and DNA replication as evidenced by exposed silver grains in the photographic emulsion. The results indicated little or no kinetochore associated DNA replication; a finding that was confirmed using BrdU incorporation and anti-BrdU antibodies (data not shown).

Kinetochore Fragmentation in MUGs

Since our investigation with CHO MUGs suggested that unreplicated kinetochores had been fragmented upon detachment from the chromosomes, we examined this further by analyzing MUGs in a cell with a low diploid chromosome complement. Chromosomes of the male Indian muntjac (2N = 7) display pairs of large compound kinetochores (Fig. 2

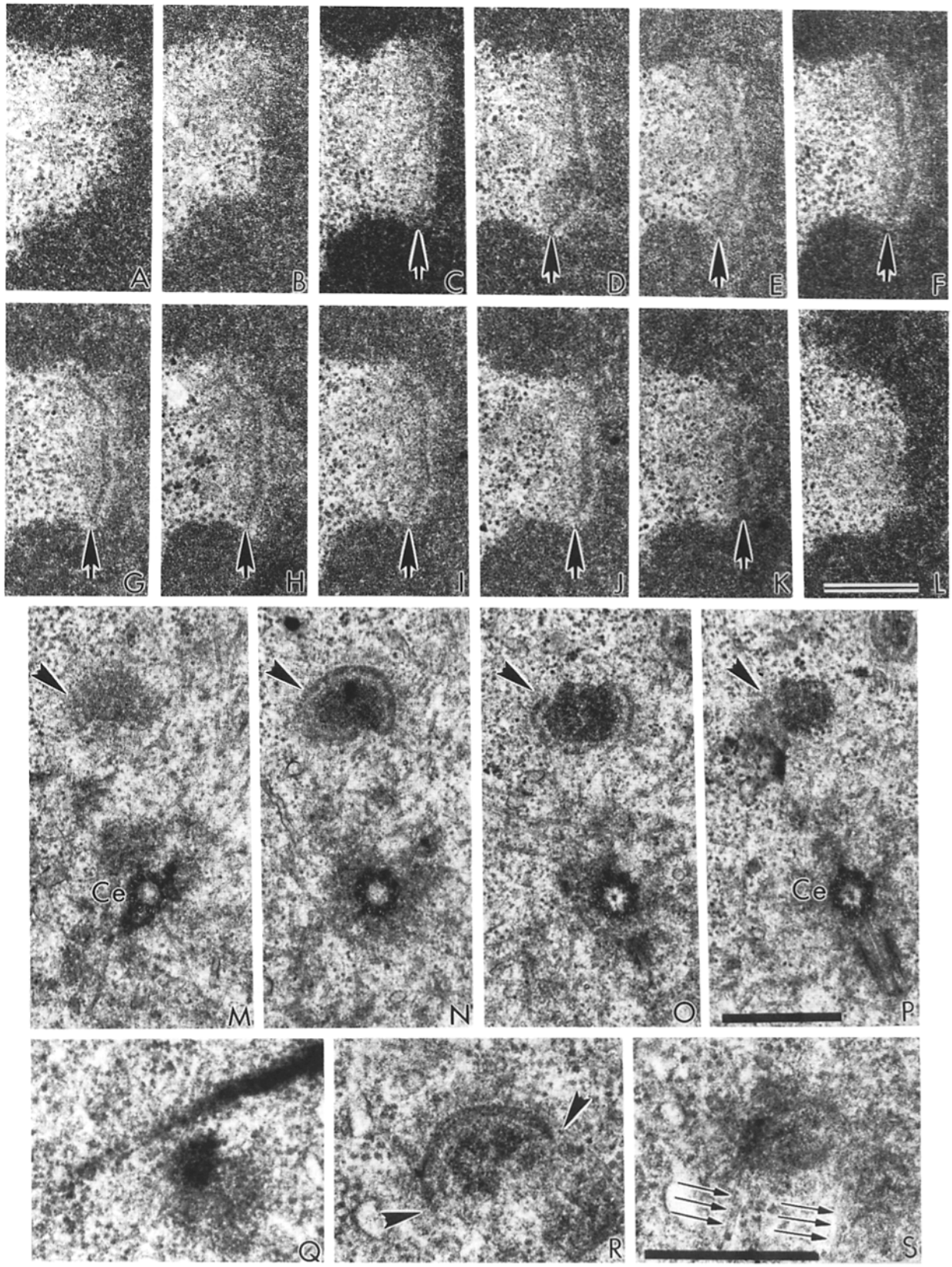

Figure 4. Serial sections of intact and detached kinetochores. (*A–L*) Serial sections of the centromere region of a normal Indian muntjac chromosome. In 9 of the 12 sections shown, the plate emerged from a condensed chromatin mass on one side of the primary constriction (*C–K, arrowheads*), extended laterally along the centromere and reinserted into the chromatin on the opposite side of the constriction. Serial sections cut through detached kinetochores (*M–P, arrowheads* and *Q–S*) show a familiar plate (*N, O,* and *R, arrowheads*) that can be followed in only one or two sections. Entire detached kinetochores can be accounted for in three to four adjacent sections. A centriole (*Ce*) can be seen in *M–P.* Arrows in *S* point to microtubules traversing to the kinetochore. Bars, 0.5 μm.

A) which presumably evolved through multiple centric and tandem chromosomal fusions from a more primitive karyotype, such as seen in the Chinese muntjac (2N = 46) (Fig. 2 *E*) (9). When Indian muntjac cells were induced to become MUGs and examined by immunofluorescence using CREST antibodies, as many as 80–100 smaller fluorescent spots were seen instead of the seven kinetochores (Fig. 2 *B*), indicating extensive fragmentation of each kinetochore. A similar situation was seen when Chinese muntjac cells were induced to become MUGs. Again, as many as 80–100 smaller fluorescent kinetochore foci were detected (Fig. 2 *F*) in each mitotic cell. As in CHO MUGs, the kinetochore fragments in both of these species were observed to interact with microtubules of the mitotic spindle (Fig. 2, *C* and *G*), whereas the highly fragmented chromatin was found dispersed peripherally in the cell (Fig. 2, *D* and *H*). Examination of muntjac MUGs by EM revealed the same characteristic kinetochore morphology seen in CHO MUGs (see Fig. 4, *M–S*).

Further evidence for kinetochore fragmentation in MUGs was obtained through digital image analysis of the respective areas of fluorescence of detached and intact kinetochores. We reasoned that if the fluorescent kinetochores seen in MUGs represented fragments and not whole kinetochores, their areas of fluorescence should be proportionately smaller than that of normal kinetochores on intact metaphase chromosomes. The fluorescent areas of intact and detached kinetochores on CHO, Chinese, and Indian muntjac chromosomes are shown in Figs. 3, *A–F* as measured by video microscopy and computer morphometrics. The mean fluorescent areas of kinetochores on CHO and Chinese muntjac chromosomes were determined to be 0.22 (range 0.09–0.35 μm^2) and 0.24 μm^2 (range 0.15–0.38 μm^2), respectively (Fig. 3, *A* and *C*). These values agree well with previously published areas of kinetochores as determined by immunofluorescence and EM (9, 14) and demonstrate the uniformity of size of these kinetochores from one chromosome to the next. When CHO and Chinese muntjac cells were induced to become MUGs, the kinetochore fragments displayed proportionately smaller mean fluorescent areas of 0.12 μm^2 (range 0.05–0.19 μm^2 for CHO MUGs; range = 0.05–0.23 μm^2 for Chinese muntjac MUGs) (Fig. 3, *B* and *D*). Thus, the fluorescent areas of MUG kinetochores were approximately one-half the fluorescent areas of kinetochores on intact metaphase chromosomes.

The evolution of Indian muntjac chromosomes by multiple centric fusions has resulted in compound kinetochores with up to a six fold variation in size (9). The characteristic morphology of the elongated kinetochore of the X chromosome makes it easy to identify in mitotic cells. Thus, it was possible to specifically measure the fluorescent area of this kinetochore and compare it with the other kinetochores in the genome. The mean fluorescent area of the X chromosome was 0.86 μm^2 (range = 0.63–1.24 μm^2), whereas the other chromosomes of the genome had a mean fluorescent area of 0.35 μm^2 (range = 0.20–0.57 μm^2) (Fig. 3 *E*). The data demonstrate the heterogeneity of kinetochore sizes observed on Indian muntjac chromosomes. When Indian muntjac cells were induced to become MUGs, the kinetochore fragments had a significantly smaller mean area of fluorescence of 0.14 μm^2 (range = 0.07–0.23 μm^2, Fig. 3 *F*). These areas were over six times smaller than the mean areas measured for the X chromosome, and over 2.5 times smaller than the mean areas measured for the rest of the genome, indicating that these large compound kinetochores became extensively fragmented. Surprisingly, the fluorescent areas and overall intensity of MUG kinetochores from all three species were very similar. This and the EM morphometric data presented below show that kinetochores from various species fragment into units of similar dimensions.

Analysis of Serial EM Sections of Intact and Detached Kinetochores

Several interesting features were seen when serial sections of metaphase chromosomes were digitized and analyzed by computer-assisted reconstruction. Shown in Fig. 4, *A–L*, are 12 contiguous 70-nm sections cut through the longitudinal axis of a metaphase chromosome of an Indian muntjac cell. In 9 of the 12 sections shown, a distinct electron-dense element, usually called the outer plate or layer can be detected. The plate emerges from a condensed chromatin mass on one side of the primary constriction (*arrowheads*, Fig. 4, *C–K*), extends laterally along the centromere and reinserts into the chromatin on the opposite side of the constriction. The plate has been described as a cohelical filament (5, 6, 17, 50) and in several of these sections, the element does resemble a helix ~5–10 nm wide. A prominent corona is observed on the outer surface of the plate and a thin electron-translucent zone ~25–30 nm wide separates the plate from the underlying centromeric chromatin. Since the sections were from a colcemid-arrested cell, no microtubules are associated with the kinetochore.

Serial sections cut through kinetochores of colcemid-arrested cells, such as the ones shown in Fig. 4, *A–L*, are difficult to interpret in three dimensions. In individual sections, the plate along with the corona has the appearance of a lampbrush-like filament as originally described by Brinkley and Stubblefield (5, 6). However, since the plate can be seen in several adjacent sections, computer-assisted reconstructed images resembled a disk (data not shown) as originally described by Jokelainen (26) and others (reviewed in references 12 and 48). When serial thin sections of detached kinetochores from MUGs were so analyzed, however, a different interpretation was possible.

Serial sections cut through detached kinetochores are shown in Fig. 4, *M–P* and *Q–S*. In Fig. 4, *M–P* a distinct plate is seen in only two out of four sections cut completely through a detached kinetochore. In some cases, the plate is seen in only a single section (Fig. 4 *R*, *arrowheads*) and the entire kinetochore, including corona and associated chromatin, is accounted for in three adjacent sections (Fig. 4, *Q–S*). It was often easy to detect the "free ends" of a plate in a single section (Fig. 4 *R*, *arrowheads*), or by analyzing two adjacent sections (Fig. 4, *N* and *O*). Such obvious boundaries allowed us to precisely measure the "length" dimension of detached kinetochores as presented below. In almost every case, the plate enclosed a central chromatin mass as described earlier. Cross-section of plates appeared as dense cores surrounded by less dense fibrils presumed to be the corona (data not shown).

Sections cut along the longitudinal axis of chromosomes, such as the ones shown in Fig. 4, *A–L*, allowed us to measure the length of the plate of intact kinetochores. The plate of Indian and Chinese muntjacs were digitized from micrographs of serial sections as described in Materials and Meth-

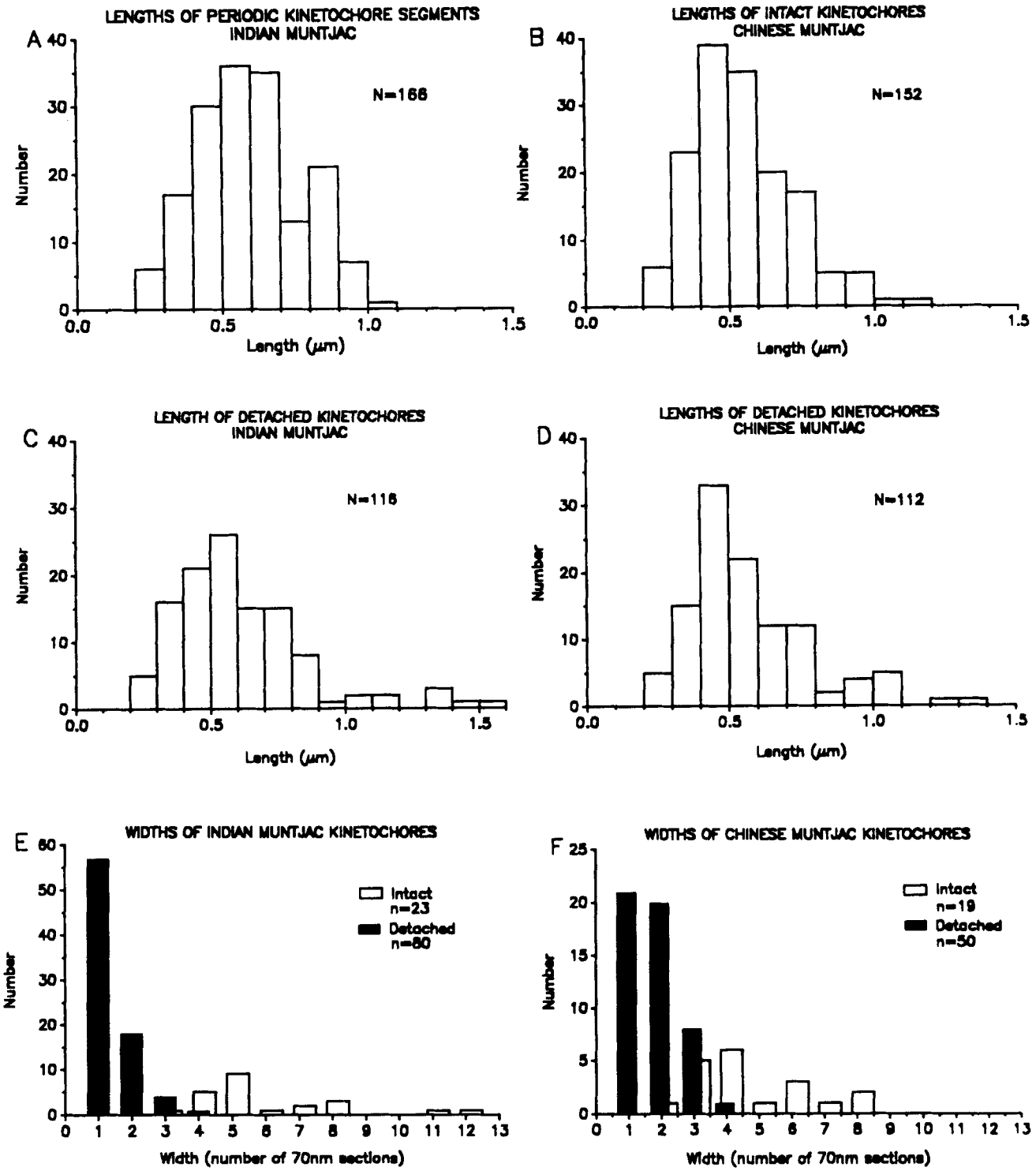

Figure 5. Lengths and widths of kinetochore plates measured by EM morphometrics. Distributions of the lengths of the electron-dense elements of intact kinetochores (*A* and *B*) and detached kinetochores (*C* and *D*) in Chinese muntjac (*B* and *D*) and Indian muntjac (*A* and *C*). The same general distributions of plate lengths were observed for both intact and detached kinetochores. (*E* and *F*) Histograms of the widths (number of 70-nm serial sections the kinetochore spans) of intact and detached kinetochores in Indian muntjac (*E*) and Chinese muntjac (*F*). The widths were determined from the same serial sections used in *A–D* to determine the plate length.

ods. Unlike the Chinese muntjac, the compound kinetochores of the Indian muntjac were unusually long but often displayed periodic discontinuities along the plate. In the case of Indian muntjac chromosomes, we measured the length of the periodic segments and not the entire compound kinetochore. As a result, the lengths of plates of intact kinetochores of the two muntjac species were very similar (Fig. 5, *A* and *B*). The mean length of the plate of Indian muntjac kinetochores was

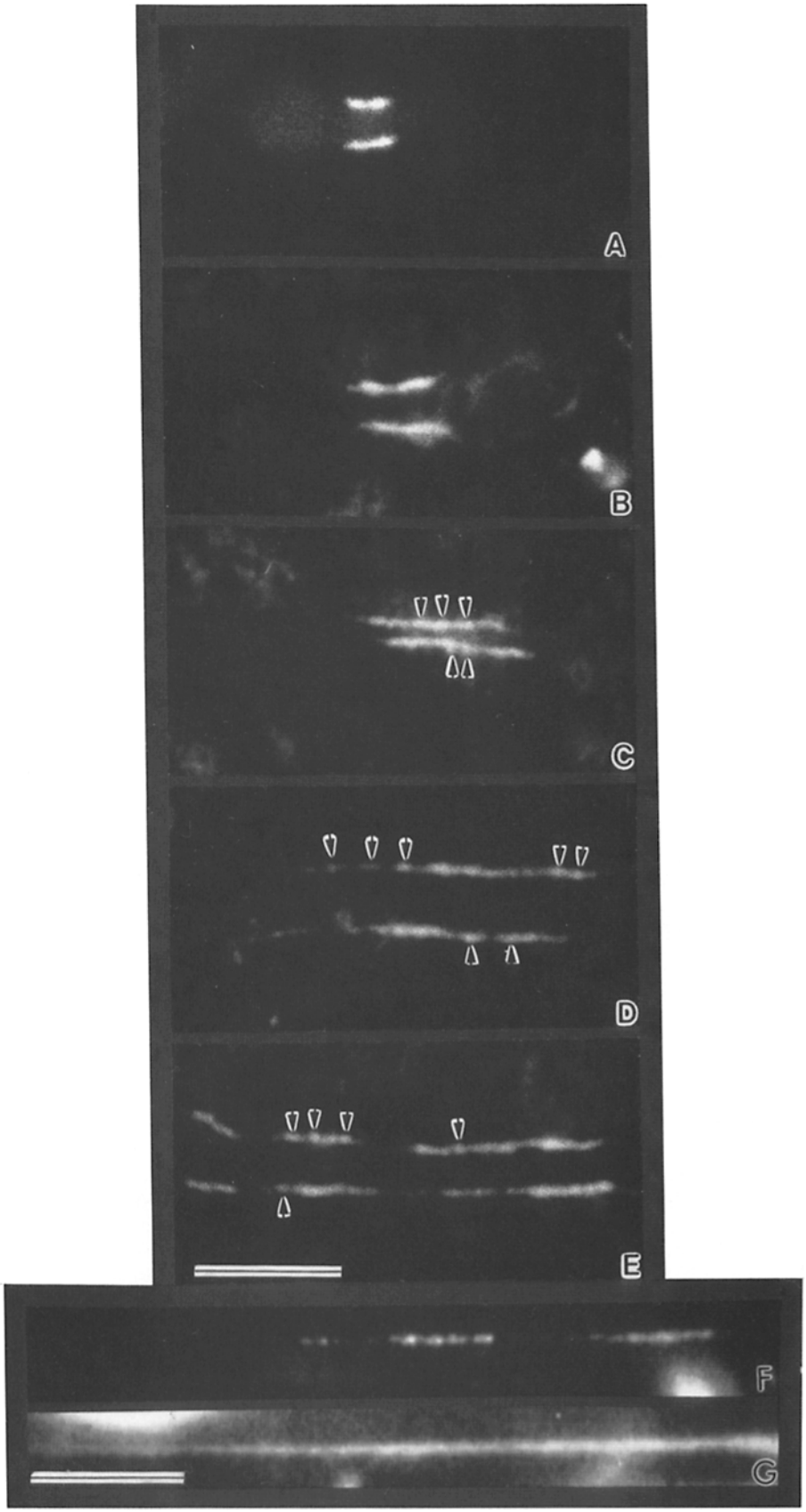

Figure 6. Hypotonic stretching of Indian muntjac kinetochores. (*A*) Normal CREST stained kinetochore on the X chromosome. (*B–F*) Hypotonically distended, CREST stained kinetochores on the X chromosome showing progressive degrees of stretching. Stretched kinetochores displayed a punctate subunit structure which became more discontinuous as the kinetochores were further stretched (*arrowheads*). The array of fluorescent subunits, such as those seen in *F* were positioned along a continuous thread of DNA as observed by Hoechst staining (*G*). Bars, 5 μm.

0.59 μm (SD = 0.20), while the mean plate length of Chinese muntjac was 0.54 μm (SD = 0.20). When the same methodology was used to measure the plates of detached kinetochores from Indian and Chinese muntjac MUGs, it was found that their lengths were also similar (Fig. 5, *C* and *D*), with the mean lengths being 0.61 μm (SD = 0.20) and 0.57 μm (SD = 0.20) respectively. Moreover, the lengths of the plates of detached kinetochores were essentially the same as their intact counterparts. The striking difference between intact and detached kinetochores was not in the length of their plates, but in the number of 70-nm serial sections it took to completely cut through a kinetochore as shown in Fig. 5, *E–F*. We refer to this dimension as the width. Thus, on the average, intact kinetochores of Indian muntjac occupied six sections (mean = 5.9), whereas the detached kinetochores of the MUGs were accounted for in one to two sections (mean = 1.4) (Fig. 5 *E*). A similar situation existed for Chinese muntjac, with intact kinetochores spanning an average of six sections (mean = 5.6), whereas the MUG kinetochores were contained within an average of one to two sections (mean = 1.8) (Fig. 5 *F*). Thus, when kinetochores became detached and fragmented, the plates retained their characteristic length, however, their widths were considerably smaller than that of the intact kinetochores. The data demonstrate that kinetochores in MUGs become fragmented into smaller units of relative uniform size.

Kinetochore Stretching

Thus far, all of our results from the analysis of detached kinetochores of MUGs suggests that the kinetochores of intact metaphase chromosomes contain repetitive subunits. Moreover, each subunit appears to be composed of DNA, as detected by Hoechst or propidium iodide staining, and protein as indicated by CREST immunofluorescence. Since caffeine alone, or in combination with, HU is known to produce DNA lesions in mammalian chromosomes (25, 52), we surmised that the detached kinetochores of MUGs arose by fragmentation of a linear DNA/protein filament that may fold into a plate- or disc-like structure. Thus, we reasoned that manually stretching the centromeres may "unfold" the kinetochore and allow us to detect linear stretches of DNA and tandem kinetochore repeats with CREST antibodies and centromeric DNA probes. We attempted to stretch kinetochores mechanically by taking advantage of shear forces generated in a cytocentrifuge, or alternatively, unraveled chromosomes by using hypotonic treatments.

The results of hypotonic induced distention of kinetochores on the X chromosomes of Indian muntjac are shown in Fig. 7. For comparison, a normal CREST-stained kinetochore (Fig. 6 *A*) and kinetochores displaying various degrees of stretching (Fig. 6, *B–F*) are shown. As can be seen in this panel, the stretched kinetochores displayed a punctate subunit structure which became more discontinuous as the kinetochores were further distended (Fig. 6, *B–F, arrowheads*). Furthermore, stretched pairs of sister kinetochores showed very similar if not identical subunit organization, as expected. In every case, when the same CREST-stained kinetochores (Fig. 6 *F*) were counter-stained with Hoechst (Fig. 6 *G*), the DNA appeared to extend continuously throughout the stretched region. Kinetochores of the other chromosomes in the muntjac genome had a similar intermittent CREST staining pattern, although due to their smaller size, attenuation resulted in kinetochores of proportionately smaller lengths.

To assess the degree of stretching produced by the hypotonic method, the lengths of normal and distended metaphase kinetochores of the Indian muntjac X chromosome were measured on immunofluorescence preparations. The mean length of normal kinetochores was 1.87 μm (range 1.51–2.64 μm), whereas the mean length of stretched kinetochores was 21.69 μm (range 9.9–39.42 μm) indicating that, on the average, the kinetochores were being stretched 11.6-fold. We actually observed that some kinetochores could be stretched >20 times their normal metaphase length.

We were also successful in stretching the centromeres of several other mammalian chromosomes, revealing a consistent repetitive pattern of subunit organization as shown in Fig. 7. For comparison, a display of normal and stretched kinetochores of CHO (Fig. 7, *A–C*) and Chinese muntjac (Fig. 7, *D–F*) are shown. We noted that the repetitive subunits of CHO kinetochores (Fig. 7, *B* and *C*) were generally more uniform in size than those seen in other species. The stretched kinetochores of Chinese muntjac chromosomes displayed a subunit pattern characteristic of Indian muntjac kinetochores, but with fewer subunits per kinetochore (Fig. 7, *E* and *F*).

A somewhat different organization was noted when HeLa chromosomes were analyzed by stretching as shown in Fig. 7, *G–I*. The distended centromeres displayed a repetitive staining pattern as seen in other species. However, partially extended centromeres displayed discrete staining of the inner centromere region between the two parallel fluorescent lines (Fig. 7 *H*, *arrow*). In more fully stretched centromeres the inner centromere staining pattern disappeared (Fig. 7 *I*).

In an earlier report, we demonstrated that the kinetochores of plant chromosomes were specifically stained using CREST autoantibodies (37). The staining pattern of metaphase chromosomes of *Haemanthus* indicated that each kinetochore was organized from several smaller units (Fig. 7 *J*, *arrows*) (27). Mechanical stretching and CREST staining of *Haemanthus* centromeres revealed that these kinetochores, like those of their mammalian counterparts, were also made up of a series of small fluorescent subunits positioned along a continuous thread of DNA (Fig. 7, *K* and *L*).

The number of fluorescent subunits observed in distended CHO kinetochores increases linearly with increased stretching of the kinetochore (Fig. 8). Since normal, unstretched CHO kinetochores are fairly uniform in size and show a single fluorescent spot when stained with autoantibodies, an increase in the length of the region and the number of stained spots per unit length argues favorably for a compact, highly folded fiber with multiple overlapping subunits being linearized by the stretching process. A similar phenomenon can be seen in Giemsa-banded metaphase chromosomes where a major chromosomal band on a highly condensed chromosome is actually composed of two or more minor bands when viewed in a less condensed state (56).

We were concerned that the hypotonic treatments needed to stretch the kinetochores might extract or alter the CREST autoantigens present in this region. However, comparative immunoblots of normal and hypotonically stretched chromosomes demonstrated the retention of the CREST antigens in the stretched chromosomes (data not shown).

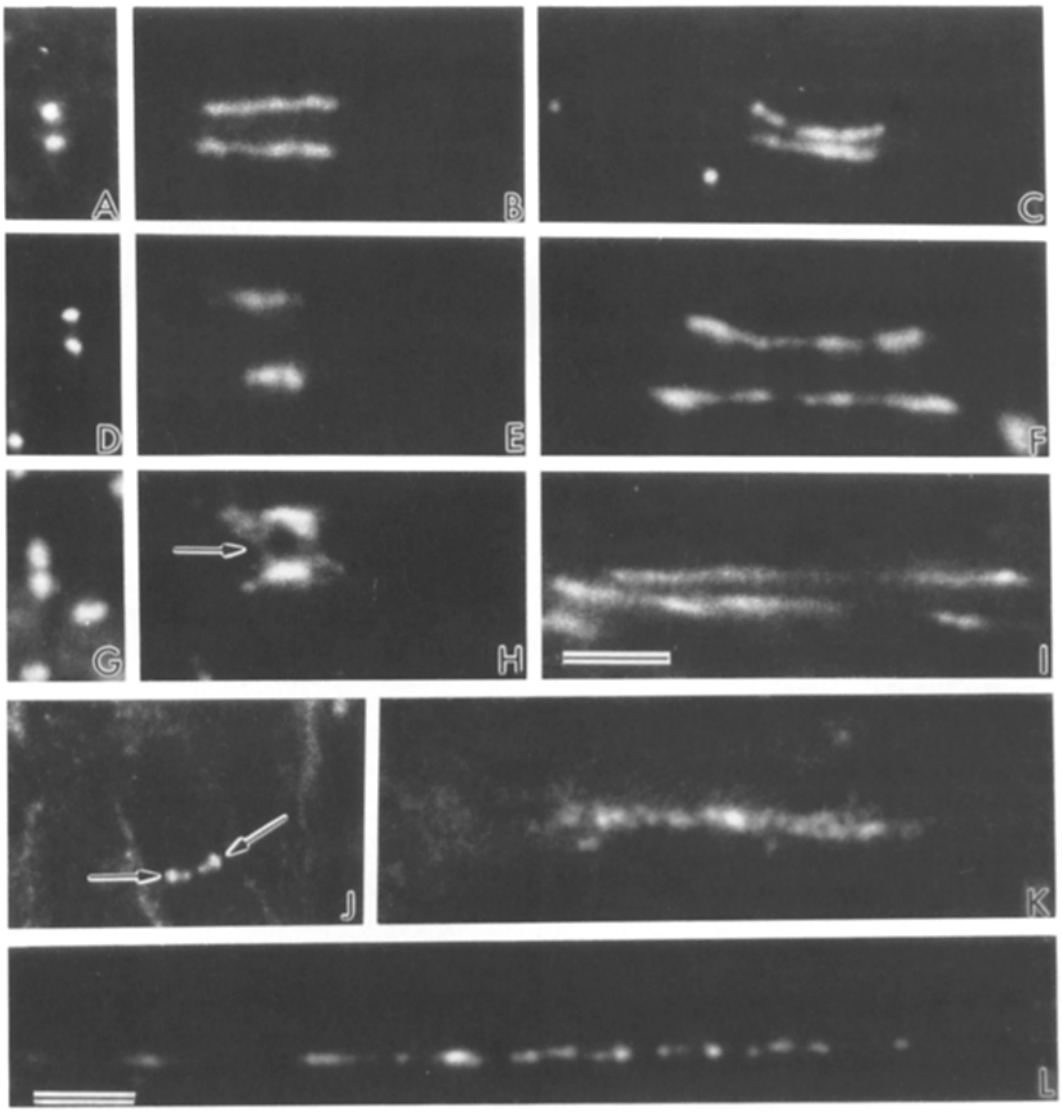

Figure 7. Hypotonic stretching of CREST stained kinetochores of CHO (*A–C*), Chinese muntjac (*D–F*), and HeLa (*G–I*), showing progressive degrees of distension. Normal kinetochores (*A*, *D*, and *G*) are shown for each of the three species. As the kinetochores became increasingly stretched the fluorescent subunits became more obvious. In partially stretched HeLa kinetochores/centromeres, discrete staining was also detected in the inner centromere region between the two parallel fluorescent lines (*H*, *arrow*) which disappeared as this region became more distended (*I*). Endosperm chromosomes from the lily *Haemanthus katherinae* Bak. stained with CREST serum displayed kinetochores that appeared to be organized from several smaller units (*J*, *arrows*). Mechanically stretched *Haemanthus* kinetochores displayed a repetitive series of small fluorescent subunits positioned along a continuous thread of chromatin (*K* and *L*). Bars, 5 μm.

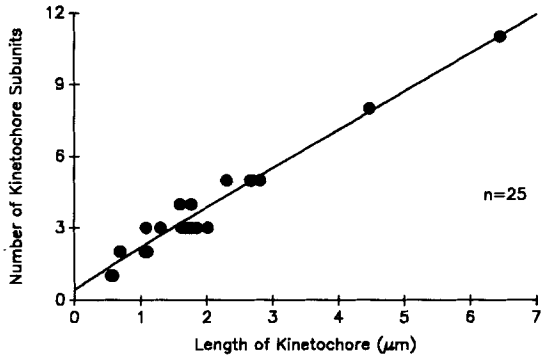

Figure 8. Subunit number versus length of stretched kinetochores: The number of fluorescent subunits observed in stretched CHO kinetochores (*ordinate*) increases linearly with increased distension of the kinetochore (*abscissa*).

In Situ Hybridization of Synthetic DNA Probes to Kinetochores and Centromeres

To establish the relationship between stretched kinetochores and their associated centromeric DNA, we combined the techniques of CREST indirect immunofluorescence with in situ hybridization using probes that recognize this class of DNA on HeLa and CHO chromosomes. HeLa chromosomes were processed for CREST immunofluorescence (Fig. 9 *A*), photographed, and then processed for in situ hybridization using a consensus sequence DNA probe that selectively hybridizes to the alphoid sequences located at the centromeres of human chromosomes (Fig. 9 *B*) (30). CREST-stained kinetochores displayed paired fluorescence spots at the lateral regions of the centromeres (Fig. 9 *A*, *arrows*). In many instances these foci were connected by a fainter band of fluores-

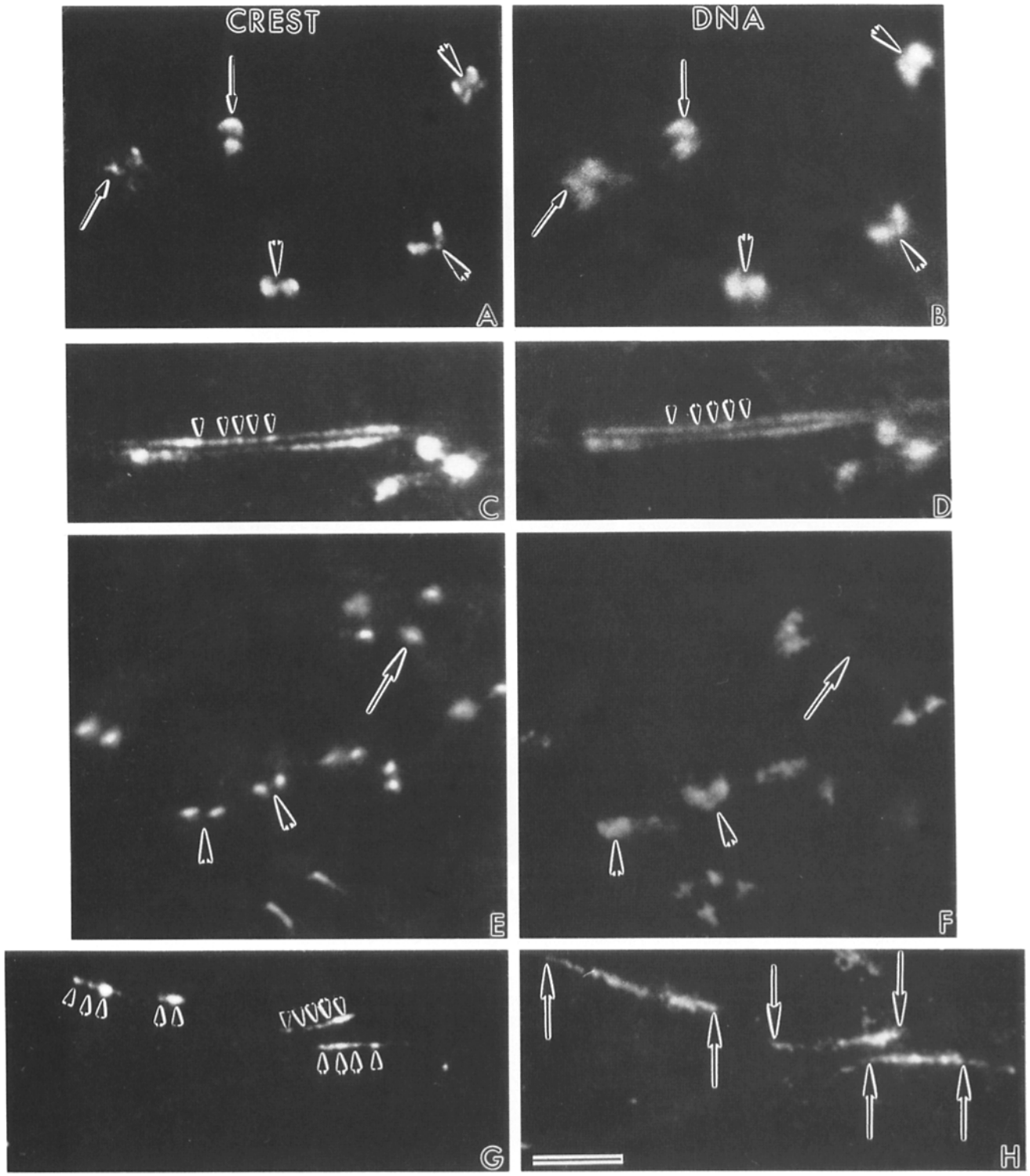

Figure 9. CREST immunofluorescence and in situ hybridization of synthetic centromere probes to HeLa and CHO chromosomes. In situ hybridization was performed using a consensus sequence DNA probe (GTTTTGAAACACTCTTTTTGTAGAATCTGC) that selectively hybridizes to the alphoid sequences located at the centromeres of human chromosomes. Normal chromosomes were stained with CREST serum (*A*) and subsequently hybridized to the biotinylated alphoid DNA probe (*B*). CREST staining produced a paired (*A*, *arrows*) or barbell appearance (*A*, *arrowheads*). Arrows and arrowheads in (*B*) correspond to those in *A*. Stretched centromere–kinetochore complexes revealed a linear array of CREST-positive subunits (*C*, *arrowheads*), with the alphoid DNA probe extending along the array (*D*). Arrowheads in *D* correspond to those in *C*. A combination of CREST indirect immunofluorescence and in situ hybridization was performed using the telomere probe $(TTAGGG)_n$ that recognizes this sequence in most of the CHO centromeres. On control chromosomes, the kinetochores appeared as discrete paired dots on the lateral edges of the primary constriction (*E*, *arrowheads*), whereas the DNA probe displayed a strong signal that spanned the entire centromere (*F*, *arrowheads*). Many of the large metacentric chromosomes stained with CREST antibodies (*E*, *arrow*), hybridized weakly or not at all with the telomere probe (*F*, *arrow*). Stretched centromere–kinetochore complexes immunostained with CREST displayed fluorescent subunits (*G*, *arrowheads*) that contained the telomere sequence as identified by in situ hybridization (*H*). In most cases the telomere probe flanked the CREST positive areas (*H*, *arrows*). Bar, 5 μm.

cence producing a barbell appearance (Fig. 9 *A*, *arrowheads*). In situ hybridization to the same chromosomes (Fig. 9 *B*) showed the centromere–kinetochore regions contained alphoid DNA that spanned an area which was inclusive of, but much larger than the area stained by CREST antibodies (compare Fig. 9, *A* with *B*).

Hypotonically stretched chromosomes displayed several consistent patterns when the CREST staining (Fig. 9 *C*) was compared with the in situ hybridization (Fig. 9 *D*). Kinetochores that became stretched revealed a linear array of subunits as seen with the CREST autoantibodies (Fig. 9 *C*, *arrowheads*), with the alphoid DNA probe extending along the array (Fig. 9 *D*, *arrowheads*). A similar pattern of staining was observed in HeLa by Masumoto et al. (29).

We performed essentially the same experiments on the kinetochore/centromere regions of normal and hypotonically stretched CHO chromosomes using the telomere probe $(TTAGGG)_n$. This sequence is also present in the centromeres of most CHO chromosomes (31, 32). Both CREST immunofluorescence (Fig. 9 *E*) and in situ hybridization (Fig. 9 *F*) are shown for comparison on the same set of normal metaphase chromosomes. Whereas the kinetochores appeared as discrete paired dots on the lateral edges of the primary constriction (Fig. 9 *E*, *arrowheads*), in situ hybridization displayed a strong signal that spanned the entire centromere region of most chromosomes (Fig. 9 *F*, *arrowheads*). Many of the large metacentric chromosomes stained with the CREST antibodies (Fig. 9 *E*, *arrow*) hybridized weakly or not at all with the DNA probe (Fig. 9 *F*, *arrow*) as previously reported (31, 32).

When CHO kinetochores were hypotonically stretched, the CREST staining again revealed a beaded pattern of fluorescence along their lengths (Fig. 9 *G*, *arrowheads*). In situ hybridization using the DNA probe showed this area to be rich in the DNA sequence (TTAGGG), that in most cases, was found in the area consisting of and flanking the CREST kinetochore probe (Fig. 9 *H*, *arrows*).

We have also used this telomeric probe on CHO MUGs, and as expected, the probe localized to most of the kinetochore-associated DNA on the metaphase plate (data not shown). Thus, most of the detached and fragmented kinetochores in CHO MUGs contained the (TTAGGG) DNA sequence.

Together, the above data demonstrate that stretched centromere–kinetochore complexes, which display a linear array of repetitive subunits as detected by CREST immunofluorescence, also contain an intact linear DNA molecule spanning the entire CREST-stained region. Moreover, the DNA we have identified with our probes not only spans the kinetochore, but generally flanks it as well. Thus, not all of the centromeric DNA was associated with kinetochore proteins detected by our CREST antiserum.

Localization of Accessory Proteins to Kinetochore Subunits

Several proteins, other than the CENP antigens, have been found associated with kinetochores in recent years. Two such proteins, tubulin and cytoplasmic dynein, have been previously reported to interact with the kinetochore during mitosis (1, 35, 36, 40, 41, 43, 55). The relationship of these proteins to the CENP antigens was investigated on both normal and stretched kinetochores using double-label immunofluorescence.

Kinetochores on isolated chromosomes from Indian muntjac cells were laminated with purified bovine 6S tubulin in a microtubule assembly buffer, fixed, and processed for double-label indirect immunofluorescence using CREST and anti-tubulin antibodies. The CREST stain was confined to the outer portion of the centromere (Fig. 10 *A*) as was the tubulin stain (Fig. 10 *B*). When these computer-enhanced video microscope images were superimposed and pseudocolored (Fig. 10 *C*), tubulin (*green*) was found situated distal to the CREST stained kinetochores (*red*). Tubulin has previously been localized by EM (40, 41, 50) and immuno-EM (35) to the outermost portion of the kinetochore, the corona, whereas immuno-EM using CREST antibodies showed these antigens to be confined to the outer and inner electron dense layers of the kinetochore plate in nonhuman species (4, 58). Thus, when compared with previous EM observations, these results demonstrate that our CREST antibodies stain the kinetochore domain rather than the chromatin associated with the inner centromere region. Moreover, this technique allows us to map the relative location of proteins within the kinetochore domain of the chromosome.

The relationship of tubulin to the CREST antigens was also determined on mechanically stretched kinetochores of the Indian muntjac that were laminated with 6S tubulin. As shown earlier, these CREST-stained kinetochores displayed the characteristic punctate staining indicative of a subunit morphology (Fig. 10 *D*). Although the tubulin fluorescence was somewhat weaker than the CREST fluorescence, the kinetochore subunits were found to be associated with tubulin in an almost one-on-one correspondence (Fig. 10 *E*). As with normal kinetochores, superimposed computer enhanced video microscope images demonstrated that the tubulin laminating the corona (*green*) of these stretched kinetochores was distal to the CREST stained (*red*) kinetochores (Fig. 10 *F*).

The association of the motor protein cytoplasmic dynein with kinetochores on Indian muntjac chromosomes was studied next. The anti-dynein mAb 70.1 recognized a triplet of 70-kD polypeptides of the light chain of cytoplasmic dynein on immunoblots of Indian muntjac whole cell lysate (data not shown), as was previously reported for CHO cells (55). Double-label immunofluorescence with the anti-dynein (Fig. 10 *H*) and CREST antibodies (Fig. 10 *G*) localized the cytoplasmic dynein to the kinetochores. Steuer et al. (55) made a similar observation although the study did not employ the same methods of immunofluorescence. Upon superimposing the two images with the computer, cytoplasmic dynein (*green*) was found distal to the CREST stained kinetochores (*red*, Fig. 10 *I*). Double-label experiments performed using the anti-dynein and anti-tubulin antibodies demonstrated the perfect colocalization of these two proteins (data not shown). It has been proposed that the motor for poleward chromosome movement is in or near the kinetochore (39). These experiments localized cytoplasmic dynein in the outer portion of the kinetochore domain that may represent the corona, the most likely site for a kinetochore associated motor (49).

Mechanically attenuated kinetochores were also double stained with CREST and anti-cytoplasmic dynein antibodies. As expected, the CREST positive subunits of the kinetochore (Fig. 10 *J*) showed a one-to-one relationship with the punctate staining pattern produced with the anti-dynein antibody (Fig. 10 *K*). This is also evident when the computer-enhanced video images are superimposed and pseudocolored (Fig. 10 *L*). Furthermore, the dynein stain (*green*) was distal

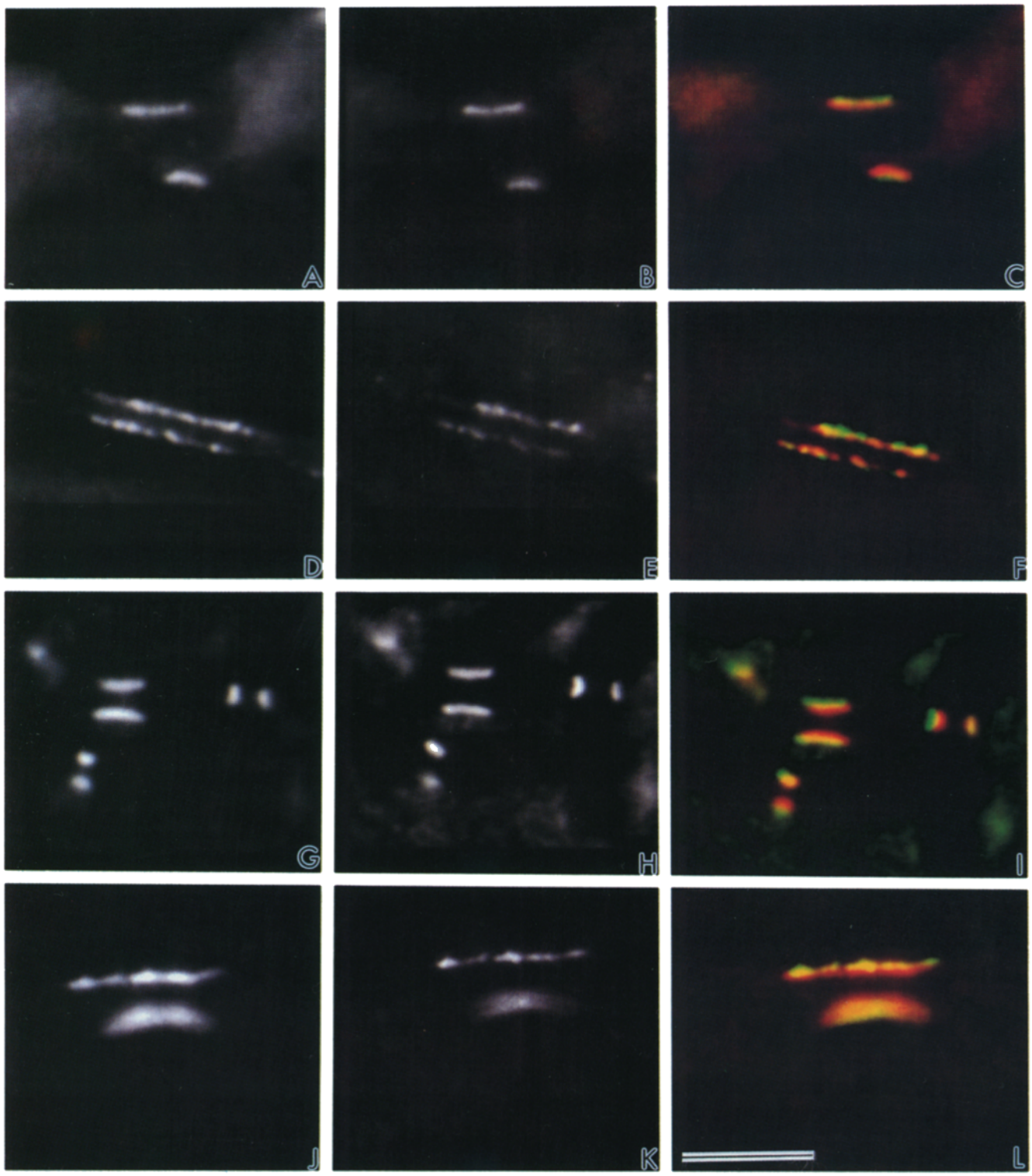

Figure 10. Localization of cytoplasmic dynein and tubulin in normal and stretched CREST-stained kinetochores. Kinetochores of chromosomes of the Indian muntjac were stained by double indirect immunofluorescence for the presence of CREST antigens and tubulin or cytoplasmic dynein and visualized with the aid of computer-enhanced video microscopy. (*A*) CREST-stained normal kinetochores. (*B*) The same kinetochores stained with tubulin antibody TU-27B. (*C*) Computer overlay of the two stains. (*Red*) CREST; (*green*) tubulin; (*yellow*) areas of overlap between the two stains. Stretched kinetochores stained with CREST antibodies (*D*) and TU-27B (*E*). Computer overlay of the two stains (*F*). In both cases the tubulin stain was located distal to the kinetochore stain. (*G*) CREST-stained kinetochores of a normal cell. (*H*) Kinetochores stained with the anti-dynein 70.1 antibody to cytoplasmic dynein. (*I*) Computer overlay of the two stains. (*red*) CREST; (*green*) cytoplasmic dynein; (*yellow*) areas of overlap. (*J*) CREST-stained stretched kinetochore. (*K*) Anti-dynein stained stretched kinetochore. (*L*) Computer overlay of the two stains. The cytoplasmic dynein stain, like the tubulin stain, was localized distal to the kinetochore stain. Bar, 5 μm.

to the CREST stain (*red*) indicating the presence of cytoplasmic dynein in the outer portion of the kinetochore domain. Hence, cytoplasmic dynein is probably associated with the corona of kinetochore subunits.

Discussion

A Common Thread in Kinetochore Evolution

Generally, kinetochores of various eukaryotic chromosomes have similar functions but vary considerably in appearance at metaphase. Mammalian chromosomes, as well as those of many other eukaryotic species have kinetochores that are localized to a single specific site, usually the primary constrictions, and display a disc or plate-like organization at metaphase. This highly conserved design is found in organisms as phylogenetically diverse as diatoms and humans. Other organisms, including chromosomes of higher plants and some insects, have localized kinetochores which depart from the trilaminar plate design and appear as a "ball and cup" at the primary constriction (12, 48). In round worms, orthopteran insects and monocotyledonous plants, the chromosomes lack a primary constriction and have diffuse or "holocentric" kinetochores extending from one end of the chromosome to the other (12, 48). In some organisms such as the budding yeast, kinetochores are not visible on mitotic or meiotic chromosome and spindle microtubules appear to attach directly to a chromatin fiber (42).

Given the diversity of structural patterns in nature, it is difficult to envision a common design that could explain the evolution of the various kinetochore types on eukaryotic chromosomes. It is equally difficult to visualize how kinetochores with such diverse morphologies are integrated into the general scheme of chromatin organization of the centromere and chromosome arms.

Is the kinetochore a separate and distinct entity organized as a proteinaceous interface between spindle microtubules and chromatin, or is it integrated into and continuous with a chromatin fiber which organizes the chromosomes of all eukaryotic cells? The data obtained in the present study support the latter interpretation. That is, regardless of its design as a condensed, localized plate or ball or linear fiber dispersed along the entire length of the chromosome, the kinetochores of all species examined thus far can be identified as short functional fragments or microtubule-binding segments arranged as discontinuous repeats along a continuous DNA fiber. Thus, the organization of kinetochores of various species appears to be a product of the degree and pattern of condensation and folding of a unit chromatin fiber that organizes the kinetochore protein into a contiguous functional mass. How many repetitive segments exist and how they are brought into register to form the various kinetochore types on eukaryotic chromosomes remains to be determined.

The Repeat Subunit Model

The sum of our evidence leads inevitably to the view that the kinetochore of higher eukaryotic chromosomes is assembled by the condensation of functionally similar, repetitive subunits arranged along a continuous DNA fiber. This modular design could explain the organization of various types of kinetochores seen in nature. The model illustrated in Fig. 11 represents the localized, plate-like kinetochore of mammalian chromosomes. Here, the duplicated G_2 centromere is shown as a pair of 30-nm DNA fibers that consist of multiple, tandemly arranged elements (depicted in the drawing as a series of spheres) that are interspersed by linker DNA segments of an undetermined length. Since these elements are capable of binding tubulin and microtubules and display the morphology of metaphase kinetochore plates by EM, we have labeled them microtubule (MT)-binding segments. When chromosome condensation occurs in mitosis, these repetitive MT-binding segments are folded and aligned into parallel register to form the outer layer of the kinetochore. These linear repetitive MT-binding segments also contain the fibrous corona, depicted as hair-like projections in the diagram. As described already, tubulin and cytoplasmic dynein were found in the kinetochore domain and are most likely associated with the corona. For simplicity, only the outer layer is shown in this model. However, additional folding would bring repeated segments destined to form the inner layer of the trilaminar structure into register. The middle translucent layer as seen by EM may represent a space between the two layers. Thus, the kinetochore could be formed from a fiber that was previously interpreted as being a solid plate or disc as described by some authors.

The familiar pattern of satellite DNA organized into families of tandem repeats throughout the centromere of most eukaryotic chromosomes thus actually reflects the underlying organization of the kinetochore, a domain of the centromere. Each repetitive block or module of the kinetochore is self-contained with a unit complement of microtubule-binding proteins and motor molecules. Individually, each module is capable of undergoing the full litany of mitotic movements. When linked in tandem and folded into a parallel series, the modules collectively form the kinetochore plate seen on many metaphase chromosomes. This compound module provides a concentrated focus for both chromosome attachment to the spindle and force production needed to assure proper chromosome segregation in mitosis and meiosis.

Several earlier studies also concluded that the kinetochore is fibrous in design. In the initial EM descriptions of Brinkley and Stubblefield (5, 6), the kinetochore was described as an axial filament with lampbrush-like loops. Comings and Okada (17) proposed that the inner layer of the kinetochore was composed of chromatin, but concluded that the outer layer represented a protein disk of nonchromatin composition. Ris and Wit (50), on the other hand, concluded that the outer layer was composed of multiple hairpin loops of 10-nm chromatin originating from the inner disk that were stacked together to form a solid outer disk 30 nm in diameter. Rattner (44–46) proposed a model based on EM studies where the inner and outer plates of the kinetochore were composed of a 30-nm fiber that was continuous with the body of the chromosome. Although these earlier models share a few similarities to our own, they fail to account for the repetitive subunit organization of the kinetochore fiber. Our model can easily account for the ability of an intact kinetochore to become detached into functional fragments by drug treatments. We believe that HU in combination with caffeine in the MUG system cause breaks in the linker segments interspersed between the microtubule-binding segments. Breaks flanking a single MT-binding segment produces a "single" fragment of unit length that associates with microtubules and becomes oriented to one pole of the spindle (mono-oriented), whereas

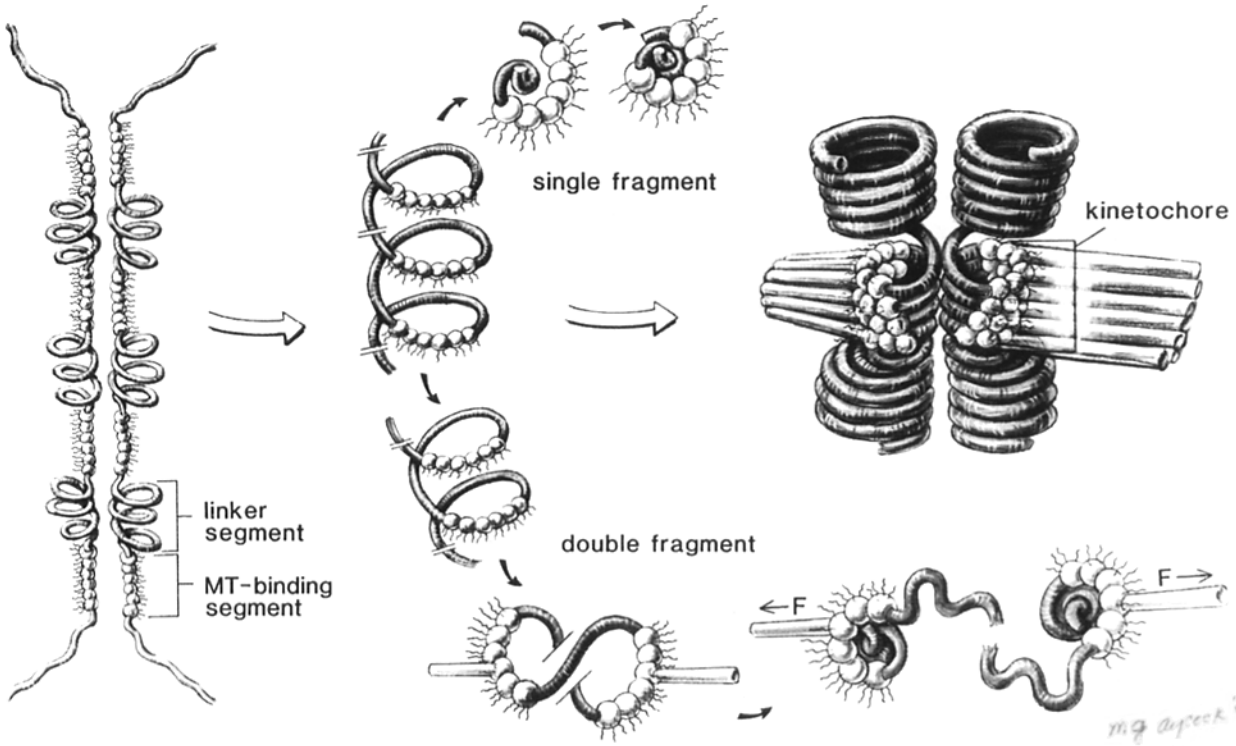

Figure 11. Model for kinetochore structure. At left, the centromere–kinetochore of a fully replicated chromosome is shown as it would appear in the G_2-phase of the cell cycle after chromosome replication. The centromere of each chromatid consists of a core 30-nm chromatin fiber which extends through the centromere and is continuous into the chromosome arms. For simplicity, the 30-nm fibers are drawn separately but in life, they would probably be bound together by inner centromere proteins (*INCENPS*) (18). The plates (MT-binding segments) are arranged as tandem repetitive domains of uniform length connected by linker segments of unknown length. Presumably, satellite DNA would form the core of this chromatin segment and a subset of nucleotide sequences would bind kinetochore proteins. In the model each globular subunit of the MT-binding segment is a complex of DNA, MT-binding proteins, and corona that might serve as an attachment site for a single microtubule. At the beginning of mitosis as shown in the center of the diagram, chromosome condensation and folding would bring the MT-binding segments together in parallel register forming a plate or disc at the primary constriction. The linker segments are folded inward to form the inner centromere. An inner plate seen on many chromosomes is not shown here but could form by additional folding or by domains associated with the underlying linker segment. Caffeine produces breaks in the DNA of the linker segments forming single or double kinetochore fragments as seen in MUGs. Double fragments can bind microtubules from each pole and become aligned and bi-oriented on the metaphase plate, resembling sister kinetochores. Single fragments appear to be mono-oriented to one pole or the other.

breaks involving two or more segments produce double fragments that become bioriented on the spindle. The bi-oriented double fragments behave as sister kinetochores and may undergo further breakage during poleward movement at anaphase, as shown in Fig. 11. Therefore, in the repeat subunit model, the length of the plate (MT-binding segment) as seen in intact metaphase kinetochores, is preserved in the detached fragments. However, the width of the kinetochore fragments is considerably reduced in comparison to the width of an intact kinetochore as would be predicted by the model.

Our model also can account for other aspects of the kinetochore region. For example, interphase kinetochores (prekinetochores [4]) can be visualized as fluorescent spots using CREST autoantibodies, but are not normally seen by EM in thin sections. Additionally, the prekinetochores in the male Indian muntjac nucleus are not visible as seven discrete spots, but instead as multiple fluorescent spots arranged in long thread-like arrays (9). A similar situation occurs for prekinetochores in Chinese muntjac (9), and the GLC1 human cell line (22). These interphase kinetochore staining patterns probably represent decondensed centromeric DNA where MT-binding segments are no longer held in precise register. This accounts for the failure to detect plate-like kinetochores in interphase nuclei by serial thin section EM or by immunoperoxidase (4) or immunogold (19) EM.

Moreover, the model proposed herein can account for experimental manipulations that bring about loss of the plate-like morphology of the kinetochore. For example, hypotonic treatment of kinetochores results in a reversible loss of the plate-like morphology (8, 50), most likely due to the swelling of chromatin fibers and disruption of MT-binding segment organization. If mammalian chromosomes are returned to an isotonic condition, they recondense and the kinetochore returns as a plate-like structure, probably due to the realignment of MT-binding segments. Additionally, chromosomes briefly treated with DNase I display a partially degraded plate composed of fibrillar material (41). The remaining portions of the plate are able to nucleate microtubules. However, prolonged treatment with DNase I abolishes both the kinetochore plate and its microtubule nucleation capability. Thus,

brief treatments with DNase I probably severed the linker regions while prolonged treatment destroyed both the linker segments and the microtubule binding segments. In short, the repeat subunit model for kinetochore structure put forth here integrates the kinetochore into the accepted pattern of chromatin organization of eukaryotic chromosomes and accounts for many previously published observations.

The model proposed herein also addresses several key aspects of chromosome evolution. The centromere–kinetochore region has been a principle site of breakage, recombination, and chromosomal rearrangement during the evolution of modern karyotypes. The present-day bi-armed chromosomes are thought to be the products of extensive centric or Robertsonian fusions between primitive telocentric elements. A highly redundant kinetochore organization involving one linear DNA molecule along the centromere could facilitate extensive breaks and exchanges, deletions, duplications, and inversions and still retain the capacity to organize into a functional kinetochore. The resilience of the centromere–kinetochore to the rigors of evolution and chromosome rearrangements may be due to the inherent redundancy of the kinetochore organizing DNA of this region. Kinetochores of eukaryotic chromosomes may have evolved from smaller "units" that have been added by recombination throughout the course of time. If so, the evolutionary history of each eukaryotic chromosome may be recorded in the number and distribution of microtubule-binding domains distributed along the centromeric DNA.

We gratefully acknowledge the efforts of medical students Jay Carpenter and Steve McCune who assisted in collecting and analyzing morphometric data in this study. We thank Ed Phillips for assistance with the EM and photography and Ric Villani for maintaining the cell cultures. Paula Gregory's assistance and advice with initial in situ investigations is also gratefully acknowledged. Appreciation is extended to Albert Tousson for technical assistance, proofreading, and helpful comments. Thanks are also extended to Changqing Zeng, Da Chang He, Ilya Uspensky, and Ron Balczon for advice and helpful discussions. We appreciate the kindness of L. I. Binder for providing TU-27B antibody against β-tubulin and Eric Steur and Mike Sheetz for their generous gift of antibody 70.1 against cytoplasmic dynein. We are grateful to William Koopman and Graciela Alarcon of the Comprehensive Arthritis Center for providing serum from scleroderma CREST patients. Special thanks are also extended to Ann Harrell for editorial assistance and Sherry Crittenden for typing the manuscript.

This research is supported by National Institutes of Health grant CA 41424 to B. R. Brinkley, and Department of Energy Contract F518/B04718 to J. Meyne.

Received for publication 1 February 1991 and in revised form 28 February 1991.

References

1. Balczon, R. D., and B. R. Brinkley. 1987. Tubulin interaction with kinetochore proteins: analysis by in vitro assembly and chemical crosslinking. *J. Cell Biol.* 105:855–862.
2. Bloom, K., and E. Yeh. 1989. Centromeres and telomeres: structural elements of eukaryotic chromosomes. *Curr. Op. Cell Biol.* 1:526–532.
3. Borland, L., G. Harauz, G. Bahr, and M. van Heel. 1988. Packing of the 30 nm chromatin fiber in the human metaphase chromosome. *Chromosoma (Berl.).* 97:159–163.
4. Brenner, S., D. Pepper, M. W. Berns, E. Tan, and B. R. Brinkley. 1981. Kinetochore structure, duplication, and distribution in mammalian cells: analysis by human autoantibodies from scleroderma patients. *J. Cell Biol.* 91:95–102.
5. Brinkley, B. R., and E. Stubblefield. 1966. The fine structure of the kinetochore of a mammalian cell *in vitro*. *Chromosoma (Berl.).* 19: 28–43.
6. Brinkley, B. R., and E. Stubblefield. 1970. Ultrastructure and interaction of the kinetochore and centriole in mitosis and meiosis. *Adv. Cell Biol.* 1:119–185.
7. Brinkley, B. R., and J. P. Chang. 1973. Embedding *in situ*. *In* Tissue Culture: Methods and Applications. Academic Press, New York. pp. 438–443.
8. Brinkley, B. R., S. M. Cox, and D. A. Pepper. 1980. Structure of the mitotic apparatus and chromosomes after hypotonic treatment of mammalian cells *in vitro*. *Cytogenet. Cell Genet.* 26:165–174.
9. Brinkley, B. R., M. M. Valdivia, A. Tousson, and S. L. Brenner. 1984. Compound kinetochores of the Indian muntjac: evolution by linear fusion of unit kinetochores. *Chromosoma (Berl.).* 91:1–11.
10. Brinkley, B. R., A. Tousson, and M. M. Valdivia. 1985. The kinetochore of mammalian chromosomes: structure and function in normal mitosis and aneuploidy. *In* Aneuploidy. V. L. Dellarco, P. E. Voytek, and A. Hollaender, editors. Plenum Publishing Corp., New York. 243–267.
11. Brinkley, B. R., R. P. Zinkowski, W. L. Mollon, F. M. Davis, M. Pisegna, M. Pershouse, and P. N. Rao. 1988. Movement and segregation of kinetochores experimentally detached from mammalian chromosomes. *Nature (Lond.).* 336:251–254.
12. Brinkley, B. R., M. M. Valdivia, A. Tousson, and R. D. Balczon. 1989. The kinetochore: structure and molecular characterization. *In* Mitosis: Molecules and Mechanisms. J. Hyams and B. R. Brinkley, editors. Academic Press, New York. pp. 77–118.
13. Broccoli, D., N. Paweletz, and B. K. Vig. 1989. Sequence of centromere separation: separation in a quasi-stable mouse-human somatic cell hybrid. *Chromosoma (Berl.).* 98:167–173.
14. Cherry, L. M., A. J. Faulkner, L. A. Grossberg, and R. Balczon. 1989. Kinetochore size in mammalian chromosomes: an image analysis study with evolutionary implications. *J. Cell Sci.* 92:281–289.
15. Clarke, L. 1990. Centromeres of budding and fission yeasts. *Trends Genet.* 6:150–154.
16. Clarke, L., and M. P. Baum. 1990. Functional analysis of a centromere from fission yeast: a role for centromere-specific repeated DNA sequences. *Mol. Cell. Biol.* 10:1863–1872.
17. Comings, D. E., and T. A. Okada. 1971. Fine structure of the kinetochore in Indian muntjac. *Exp. Cell Res.* 67:97–110.
18. Cooke, C. A., M. M. S. Heck, and W. C. Earnshaw. 1987. The inner centromere protein (INCENP) antigens: movement from the inner centromere to midbody during mitosis. *J. Cell Biol.* 105:2053–2067.
19. Cooke, C. A., R. B. Bernat, and W. C. Earnshaw. 1990. CENP-B: a major human centromere protein located beneath the kinetochore. *J. Cell Biol.* 110:1475–1488.
20. Earnshaw, W. C., and N. Rothfield. 1985. Identification of a family of human centromere proteins using autoimmune sera from patients with scleroderma. *Chromosoma (Berl.).* 91:313–321.
21. Fitzgerald-Hayes, M. 1987. Yeast centromeres. *Yeast.* 3:187–200.
22. Haaf, T., and M. Schmid. 1989. Centromeric association and non-random distribution of centromeres in human tumor cells. *Hum. Genet.* 81:137–143.
23. Hayden, J. H., S. S. Bowser, and C. L. Rieder. 1990. Kinetochores capture astral microtubules during chromosome attachment to the mitotic spindle: direct visualization in live newt lung cells. *J. Cell Biol.* 111:1039–1045.
24. Heath, I. B. 1980. Behavior of kinetochores during mitosis in the fungus *Saprolegniferax*. *J. Cell Biol.* 84:531–546.
25. Ishida, R., M. Kozaki, and T. Takahashi. 1985. Caffeine alone causes DNA damage in Chinese hamster ovary cells. *Cell Struct. Funct.* 10:405–409.
26. Jokelainen, P. T. 1967. The ultrastructure and spatial organization of the metaphase kinetochore in mitotic rat cells. *J. Ultrastruct. Res.* 19:19–44.
27. Lima de Faria, A. 1956. The role of the kinetochore in chromosome organization. *Hereditas.* 42:85–160.
28. Masumoto, H., H. Masukuta, Y. Muro, N. Nozaki, and T. Okazaki. 1989. A human centromere antigen (CENP-B) interacts with a short specific sequence in alphoid DNA, a human centromeric satellite. *J. Cell Biol.* 109:1963–1973.
29. Masumoto, H., K. Sugimoto, and T. Okazaki. 1989. Alphoid satellite DNA is tightly associated with centromere antigens in human chromosomes throughout the cell cycle. *Exp. Cell Res.* 181:181–196.
30. Meyne, J., G. Littlefield, and R. K. Moyzis. 1989. Labeling of human centromeres using an alphoid DNA consensus sequence: application to the scoring of chromosome aberrations. *Mutat. Res.* 226:75–79.
31. Meyne, J., R. L. Ratliff, and R. K. Moyzis. 1989. Conservation of the human telomere sequence $(TTAGGG)_n$ among vertebrates. *Proc. Natl. Acad. Sci. USA.* 89:7049–7053.
32. Meyne, J., R. J. Baker, H. H. Hobart, T. C. Hsu, O. A. Ryder, O. G. Ward, J. E. Wiley, D. H. Wurster-Hill, T. L. Yates, and R. K. Moyzis. 1990. Distribution of non-telomeric sites of the $(TTAGGG)_n$ telomeric sequence in vertebrate chromosomes. *Chromosoma (Berl.).* 99:3–10.
33. Miller, J. M., W. Wang, R. Balczon, and W. L. Dentler. 1990. Ciliary microtubule capping structures contain a mammalian kinetochore antigen. *J. Cell Biol.* 110:703–714.
34. Mitchison, T., and M. Kirschner. 1984. Microtubule assembly nucleated by isolated centrosomes. *Nature (Lond.).* 312:232–237.
35. Mitchison, T. J., and M. W. Kirschner. 1985. Properties of the kinetochore *in vitro*. I. Microtubule nucleation and tubulin binding. *J. Cell Biol.* 101:755–765.

36. Mitchison, T. J., and M. W. Kirschner. 1985. Properties of the kinetochore *in vitro*. II. Microtubule capture and ATP-dependent translocation. *J. Cell Biol.* 101:766–777.
37. Mole-Bajer, J., A. S. Bajer, R. P. Zinkowski, R. D. Balczon, and B. R. Brinkley. 1990. Autoantibodies from a patient with scleroderma CREST recognized kinetochores of the higher plant *Haemanthus*. *Proc. Natl. Acad. Sci. USA.* 87:3599–3603.
38. Moroi, Y., C. Peebles, M. J. Fritzler, J. Steigerwald, and E. M. Tan. 1980. Autoantibody to the centromere (kinetochore) in scleroderma sera. *Proc. Natl. Acad. Sci. USA.* 17:1627–1631.
39. Nicklas, R. B. 1989. The motor for poleward chromosome movement in anaphase is in or near the kinetochore. *J. Cell Biol.* 109:2245–2255.
40. Pepper, D. A., and B. R. Brinkley. 1979. Microtubule initiation at kinetochores and centrosomes in lysed mitotic cells: inhibition of site-specific nucleation by tubulin antibody. *J. Cell Biol.* 82:585–591.
41. Pepper, D. A., and B. R. Brinkley. 1980. Tubulin nucleation and assembly in mitotic cells: evidence for nucleic acids in kinetochores and centrosomes. *Cell Motil.* 1:1–15.
42. Peterson, J. B., and H. Ris. 1976. Electron-microscopic study of the spindle and chromosome movement in the yeast *Saccharomyces cerevisiae*. *J. Cell Sci.* 22:219–242.
43. Pfarr, C. M., M. Cour, P. M. Grissom, T. S. Hays, M. E. Porter, and J. R. McIntosh. 1990. Cytoplasmic dynein is localized to kinetochores during mitosis. *Nature (Lond.).* 345:263–265.
44. Rattner, J. B. 1986. Organization within the mammalian kinetochore. *Chromosoma (Berl.).* 93:515–520.
45. Rattner, J. B. 1987. The organization of the mammalian kinetochore: a scanning electron microscope study. *Chromosoma (Berl.).* 95:175–181.
46. Rattner, J. B., and D. P. Bazett-Jones. 1989. Kinetochore structure: electron spectroscopic imaging of the kinetochore. *J. Cell Biol.* 108:1209–1219.
47. Rieder, C. L. 1979. Localization of ribonucleoprotein in the trilaminar kinetochore of PtK. *J. Ultrastruct. Res.* 66:109–119.
48. Rieder, C. L. 1982. The formation, structure, and composition of the mammalian kinetochore and kinetochore fiber. *Int. Rev. Cytol.* 29:1–58.
49. Rieder, C. L., S. P. Alexander, and G. Rupp. 1990. Kinetochores are transported poleward along a single astral microtubule during chromosome attachment to the spindle in newt lung cells. *J. Cell Biol.* 110:81–95.
50. Ris, H., and P. L. Witt. 1981. Structure of the mammalian kinetochore. *Chromosoma (Berl.).* 82:153–170.
51. Roos, U.-P. 1973. Light and electron microscopy of rat kangaroo cells in mitosis. II. Kinetochore structure and function. *Chromosoma (Berl.).* 41:195–220.
52. Sawecha, J., B. Goos, and J. Malec. 1987. Modification by caffeine of acute cytotoxic response of cultured L5178Y cells to hydroxyurea treatment. *Neoplasma. (Berl.).* 23:369–377.
53. Schlegel, R., and A. B. Pardee. 1986. Caffeine-induced uncoupling of mitosis from the completion of DNA replication in mammalian cells. *Science (Wash. DC).* 232:1264–1266.
54. Schlegel, R., and A. B. Pardee. 1987. Periodic mitotic events in the absence of DNA replication. *Proc. Natl. Acad. Sci. USA.* 84:9025–9029.
55. Steuer, E. R., L. Wordeman, T. A. Schroer, and M. P. Sheetz. 1990. Localization of cytoplasmic dynein to mitotic spindles and kinetochores. *Nature (Lond.).* 345:266–268.
56. Sumner, A. T. 1976. Banding as a level of chromosome organization. *In* Current Chromosome Research. K. Jones, P. E. Brandham, editors. Elsevier/North Holland Biomedical Press, Amsterdam. 17–22.
57. Valdivia, M. M., and B. R. Brinkley. 1985. Fractionation and characterization of the kinetochore from mammalian metaphase chromosomes. *J. Cell Biol.* 101:1124–1134.
58. Valdivia, M. M., A. Tousson, and B. R. Brinkley. 1986. Human antibodies and their use for the study of chromosome organization. *Methods Achiev. Exp. Pathol.* 12:200–223.
59. Waye, J. S., and H. F. Willard. 1989. Concerted evolution of alpha satellite DNA: evidence for species specificity and a general lack of sequence conservation among alphoid sequences of higher primates. *Chromosoma (Berl.).* 98:273–279.
60. Willard, H. F., and J. S. Waye. 1987. Hierarchical order in chromosome-specific human alpha satellite DNA. *Trends Genet.* 3:192–198.
61. Young, S. J., S. M. Royer, P. M. Groves, and J. C. Kinnamon. 1987. Three-dimensional reconstructions from serial micrographs using the IBM-PC. *J. Electr. Microsc. Techn.* 6:207–217.
62. Zinkowski, R. P., S. McCune, R. D. Balczon, P. N. Rao, and B. R. Brinkley. 1989. The centromere and aneuploidy. I. Caffeine-induced detachment and fragmentation of kinetochores of mammalian chromosomes. *In* Mechanisms of Chromosome Distribution and Aneuploidy. M. Resnick, and B. K. Vig, editors. Alan R. Liss, Inc., New York. pp. 43–60.
63. Zinkowski, R. P., S. L. McCune, R. D. Balczon, P. N. Rao, and B. R. Brinkley. 1990. The centromere and aneuploidy. II. Drug induced detachment and fragmentation of kinetochores of mammalian chromosomes. *In* Mutation and the Environment. Part B. Metabolism, Testing Methods, and Chromosomes. M. L. Mendelsohn and R. J. Albertini, editors. Alan R. Liss, Inc., New York. 223–236.